



Migratory analysis of PM₁₀ and O₃ pollutants between urban and rural areas using functional data: EVIDENCE from Catalonia

Alejandro Betancourt¹ · Eszter Wirth² · Santiago Budría³

Received: 17 January 2022 / Accepted: 8 June 2022 / Published online: 27 June 2022
© The Author(s), under exclusive licence to Springer Nature B.V. 2022

Abstract

This paper analyzes the relationship between rural, urban, and suburban areas relative to PM₁₀ and O₃ pollution levels within the Spanish Autonomous Community of Catalonia (CC), characterized by a complex orography, and unequal population and industrial distribution. To diagnose significant correlations between these areas, this article uses functional data in conjunction with functional Kendall's tau statistic, which acknowledges the continuous nature of the variables and avoids several simplifying hypotheses that are imposed by other quantitative methods. These features are valuable in a context where the variable of interest, pollution, exhibits a large degree of dispersion over time and seasons. Data have been collected from 44 air monitoring stations on an hourly basis within the CC between the years 2013 and 2020. According to the results, remote urban and rural places often displayed a high correlation for both O₃ and PM₁₀, while some adjacent areas featured low correlations. This phenomenon should be attributed to complex recirculation patterns within the CC, where the regions of Reus, Amposta, and Constantí (located in Tarragona province) and the Vic and Berga Plains (an area of intense economic activity in the north of the Barcelona Metropolitan Area) exert strong influences on air pollution at rural sites. Regional wind flows and Saharan dust episodes may exacerbate these effects. The findings offer implications for environmental policy: policymakers should focus on the entire CC when mitigating pollution, not just Barcelona and Tarragona cities as rural sites are damaged by polluted air masses generated in urban regions.

Keywords Air pollution · PM₁₀ and tropospheric ozone · Correlation analysis · Functional data · Functional Kendall tau · Urban areas and rural areas · Air recirculation

Introduction

The World Health Organization (WHO) has provided evidence of the effects of air pollution on human health, at concentrations even lower than those established by WHO in 2005. Every year, approximately seven million premature deaths and millions of healthy life year losses can be attributed to exposure to polluted air according to this specialized agency of the United Nations (WHO 2020).

The emission of tropospheric ozone (O₃) and particulate matter (PM) is considered a serious threat for its contribution to global warming, for being a menace to marine and terrestrial ecosystems, as well as to people's health and well-being through problems of water and food security, plant damage, and migrations caused by drought and floods. According to research results, in 2019, about 90% of the world's population lived in areas where concentrations exceeded air quality thresholds established by WHO in 2005 (Guarin et al. 2019; WHO 2020).

Long-term exposure to high levels of O₃ and PM increases the probability of suffering from chronic respiratory and cardiovascular diseases (McDonnell et al. 2010; WHO 2013; Chen et al. 2018; Rohr 2018; Orellano et al. 2020). Even short-term exposure to these pollutants can lead to decreased lung mucociliary function and trigger asthma exacerbations (Karthik et al., 2017; Cesari et al. 2018). Moreover, studies have suggested that long-term exposure to pollutants is associated with both reduced

✉ Alejandro Betancourt
mabetancourt@comillas.edu

¹ Department of Quantitative Methods, Universidad Pontificia Comillas, Madrid, Spain

² Department of Economics, Universidad Pontificia Comillas, Madrid, Spain

³ Department of Economics and Business Administration, Universidad Antonio de Nebrija, Madrid, Spain

survival and life expectancy in the order of 1–2 years (Dedoussi et al. 2020). Other recent researchers have shown that the prevalence of bronchitis symptoms in children and adults is associated with exposure to PM (Amoatey et al. 2021; Yan et al. 2021). According to Ortiz-González et al. (2018), about 16,400 premature passings can be caused by tropospheric O₃ pollution in the European Union, out of which 1,700 correspond to Spain. However, almost 80% of O₃ and PM-related deaths could be avoided worldwide if current levels of air pollution were reduced to those proposed in the updated guideline, according to an analysis conducted by WHO (WHO 2021).

Traditionally, particulate air pollution has been considered to be mainly an urban phenomenon. It is now clear that, in many areas of Europe, the differences between urban and rural areas in terms of PM₁₀ are small or even non-existent, indicating that exposure to particulate matter is widespread due to, among other issues, the actions of climatological variables that enable the transport of these particles over very long distances (Rodríguez et al. 2004).

The atmospheric PM is made up of solid and/or liquid particles, which enter the atmosphere by natural pathways or through anthropogenic activities. This pollutant may present different natura: natural resuspension (by means of marine and mineral sources), biomass burning, coal combustion, road dust, traffic, industrial emissions, or heating generated by households and enterprises (Rodríguez et al. 2004; Hopke et al. 2020).

Tropospheric O₃ is a secondary atmospheric pollutant with strong oxidizing attributes. It is produced by the photooxidation of volatile organic compounds (VOCs) in the presence of nitrogen oxides (NO_x) and sunlight, but in a non-linear manner, which turns O₃ forecasting and control into a challenging task for policymakers (Atkinson 2000; Wang et al. 2016). Sillman and He (2002) outline ozone chemistry depending on these two main precursors. When the VOCs/NO_x ratio is low, then the O₃ production regime is said to be VOC-limited, and an increase (decrease) in NO_x may lead to a drop (growth) in O₃ concentrations. This kind of regime is more common in urban areas. By contrast, if the VOCs/NO_x ratio is high, then the O₃ production regime is considered to be NO_x-limited, and an increase in NO_x may lead to higher O₃ levels. This regime is more common in rural areas located downwind from emission sources, as precursors are transported by local and regional air mass flows away from urban sites (Ortiz-González et al. 2018). Moreover, high biogenic hydrocarbon levels emitted by forests and other vegetations also contribute to O₃ formation (Calfapietra et al. 2013). Consequently, adjacent rural areas tend to display more prominent O₃ levels than urban agglomerations.

Other factors that favor tropospheric O₃ generation are the following ones:

- High temperatures and strong solar radiation (Crutzen 1973; Monks et al. 2015; Guo et al. 2016), which explain why daily O₃ concentrations are the highest at midday-afternoon and during summer.
- Large wildfires, which are also prone to happen in summer (Yang et al. 2015).
- Low humidity and precipitation scarcity (Doherty et al. 2013).
- Meso-meteorological recirculations of air masses through winds and sea breezes in mountainous ranges that favor stagnation episodes of polluted air masses (Querol et al. 2016; Finardi et al. 2018).
- Economic growth (Hilboll et al. 2013).
- Global warming through rising emissions of greenhouse gases and methane (Fiore et al. 2015; Lin et al. 2017).

The circulation and redistribution of O₃ and PM across the planet is a phenomenon that poses a serious challenge to governments and health organizations when drafting air quality policies. Several articles have assessed the sources and migration of atmospheric pollutants at rural and urban sites and some of them have shown significant differences in trends and levels over time (Rodríguez et al. 2004; Paoletti et al. 2014; Jaén et al. 2021). However, there is a lack of a comprehensive analysis at local level that explicitly analyzes the migration and behavior of O₃ and PM₁₀ pollution between localities. Zong et al. (2018) are the only ones who carried out research which is similar to the one regarding O₃. An observation-based model was proposed in their paper to analyze the relationship between O₃ levels in the Chinese Shandong province's capital city and a downwind rural region. According to their results, regional air mass transport is responsible for more than 50% of the observed accumulation of O₃ in Chinese rural areas.

The Western Mediterranean Basin (WMB) is among the most exposed ones to PM and O₃ pollution in Europe according to the Intergovernmental Panel on Climate Change (2014) and the European Environmental Agency (2020) due to its abrupt orography and potential emission sources of VOCs in the urbanized and industrialized coastal and forested areas (Castell et al. 2008; Seco et al. 2011; Escudero et al. 2014). Moreover, multiple factors favor these pollutants' latter stagnation-recirculation episodes within the region (Querol et al. 2001; Rodríguez et al. 2003; Cristofanelli and Bonasoni 2009; Valverde et al. 2016).

First of all, the Mediterranean-type climate, characterized by hot summers with high temperatures, low winds and precipitations, and strong solar radiation, favors O₃ formation (Millán et al. 1997). Second, Saharan dust outbreaks (commonly known as *calima*) transport African dust to South Europe and substantially increase PM₁₀ levels, especially in summer and in winter-spring (Rodríguez et al. 2002; Rodríguez et al. 2004; Michelot et al. 2016). In third place, O₃

is subject to long-range transport towards the Mediterranean basin from Central and Eastern Europe, North America, and Asia (Lelieveld et al. 2002; Auvray and Bey 2005; Boudjella et al. 2017). Fourth, intense sea breeze dynamics are common along the shore during March–September, which contribute to PM increases in coastal regions and the transport of O₃ to inner areas (Querol et al. 2004). Fifth, the presence of important urban concentrations and economic activities on the coastal areas, such as tourism, transport, traffic, and construction, contribute to PM emissions and represent a source of NO_x and VOCs, which enhance O₃ formation. Finally, a complex geographical setup comprised of several mountainous ranges (the Alps, Apennines, Atlas, Betic, Iberian, and Catalan Ranges) favors the stagnation and recirculation of polluted air masses that get trapped within the region (Millan et al. 2000; Gangoiti et al. 2001; Rodriguez et al. 2002; Van-Drooge and Grimalt 2015; Largeron and Staquet 2016; Querol et al. 2016, 2017, 2018).

Related to O₃, despite a wide set of proven evidence, public authorities have undertaken a limited number of measures to tackle atmospheric ozone air pollution, and their main efforts have been focused on PM_{2.5} and NO₂ pollutants. PMs are composed of those with aerodynamic size below 10 µm (PM₁₀) and the fine particles with aerodynamic size below 2.5 µm (PM_{2.5}). Both can be inhaled with some depositing through the airways, but due to its size, fine PM_{2.5} has a higher likelihood to get into deeper parts of the lung, while PM₁₀ is more prone to deposit on the surfaces of the larger airways. Thus, PM_{2.5} poses a higher risk to human health compared to larger particulate matters. Moreover, the number of premature deaths associated with PM_{2.5} and NO₂ pollutants surpasses that attributed to O₃ (for instance, 27,900 and 8,900 against 1,800 in 2015, respectively; Ortiz-González et al. 2018) and the former have more intense effects on the Spanish healthcare expenses (WHO Regional Office for Europe 2015). In addition, O₃ concentrations are higher in more remote rural areas with low population, despite the fact that its precursors are generally produced at urban and industrial sites. The lack of interest in O₃ control at rural sites could be explained by data scarcity at a local level and a limited number of articles centered on O₃ dynamics in these zones.

Metropolitan areas generally concentrate on road traffic emissions and polluting economic activities that emit most atmospheric pollutants; therefore, the bulk of research has focused on their effects on urban inhabitants (Striebig et al. 2019). Nevertheless, rural areas may also register high pollution levels and be related to emissions generated at urban sites.

In the case of PM₁₀, there is a greater number of results within the CC compared to O₃ in the last 5 years. However, most of the articles only consider a specific number of localities as their study areas within the CC. However, the lack of a detailed local analysis of O₃ and PM₁₀ pollution behavior

between apparently different areas could help establish similar environmental policies between these zones, and thus optimize the use of the resources employed to reduce atmospheric pollution at all sites.

This article aims at shedding more light on the aforementioned issue. Towards this end, hourly data on O₃ and PM₁₀ pollution concentrations were extracted from 44 and 18 air monitoring stations, respectively, which cover the whole CC during the period 2012–2020.

Our article adds new insights to the existing literature along several dimensions. First, most analyses on air pollution have tracked the dynamics of O₃ and PM₁₀ by geographical zones, focusing on the effects of meteorology, seasons, calendar effects, atmospheric and air recirculation dynamics, and altitude (Paoletti et al. 2014; Porter et al. 2014; Klein et al. 2017; Querol et al. 2018). As rural sites are prone to exhibit higher mean O₃ and PM₁₀ concentrations compared to metropolitan agglomerations despite fewer pollution sources, literature started to place more emphasis on this issue. Nevertheless, 8 years have rarely been considered to study this relationship. A few papers report evidence of noticeable transfers and dynamic effects among rural and urban sites, though these links are case-specific (Rovira et al. 2018; Zong et al. 2018; Yan et al. 2019; Jaén et al. 2020) and are difficult to apply to other geographical areas. Therefore, our paper selected a specific Spanish region for this purpose, the CC.

Second, and closely related to the previous point, a more accurate detection of the major sources of air pollution at a local level can mitigate the number of deaths caused by harmful air quality. Nonetheless, because of data scarcity and the paucity of longitudinal and precise pollution measures over a significant range of geographical scenarios, it is challenging to find evidence regarding this issue. In addition, the control of O₃ and PM₁₀ turns more complicated as both pollutants depend on complex precursors and are affected by both local and distant sources (Wang et al. 2016; Xue et al. 2016; Zong et al. 2018). This paper traces significant correlations regarding O₃ and PM₁₀ pollutants between Catalan sites by counting on more than 180,000 observations (from each station) collected over 8 years from 44 and 18 air quality monitoring stations, respectively. Health authorities can use these findings to outline effective measures to develop more successful environmental policies and reduce citizens' exposure to poor air quality. As economic activities in Catalan rural areas, such as Montsec, depend on a large extent on leisure and tourism coming from several parts of Spain, high O₃ levels registered at these sites are an additional matter of concern.

Third, this article assesses the relationship between three types of sites based on orography (urban, suburban, rural) using functional data based on functional Kendall's tau (FKT), developed by Valencia et al. (2019). This approach

accepts the continuous nature of the variable that is the object of analysis and avoids several simplifying hypotheses which are typically imposed by other quantitative methods, such as multivariate regression, principal component analysis, and analysis of variance. In particular, the FKT approach provides three pros: it does not assume normality for the data of interest; it is largely insensitive to outliers; and it is able to handle nonlinear relationships. These features are valuable in a context where the variable of interest, a pollution measure, exhibits a large degree of dispersion over time and seasons. The availability of hourly pollution data during 8 years and covering the entire territory of the CC, under the umbrella of statistics used on functional data, should be able to reveal those areas with similarities in pollution behavior, all to establish more efficient environmental policies. Environmental assessment (Martínez et al. 2014; Martínez et al. 2020) and medical research (Dannenmaiera et al. 2020) are two fields where functional data analysis has been applied (Li and Chow 2005).

The selection of ozone and PM₁₀ is justified firstly by the close relationship between both pollutants in their formation process and secondly by the environmental impact that this link produces for the CC.

Material and methods

Study area and data selection

CC is a Spanish autonomous community located in the northeast of the Iberian Peninsula, bordered by France and Andorra to the north, the autonomous communities of Aragon to the west, and Comunidad Valenciana to the south. To the east, it is bordered by the Mediterranean Sea. Its territory of 32,107 km² is divided into four provinces and its capital city is Barcelona, Spain's second most populated municipality. Most of its 7.7 million inhabitants are located in the coastal plains and approximately 95% of them are concentrated in urban areas (municipalities above 200 inhabitants) according to the Catalan Regional Government (Generalitat de Catalunya 2021). The community has experienced substantial population growth rates between 2016 and 2020 compared to those of Spain and the EU average, and its regional GDP represented 19.3% of the Spanish total GDP.

Catalonia is characterized by a very complex topography, made up of high mountains, inland depressions, and a 580-km-long coastline. Such diverse orography exerts a remarkable influence on climate and pollution.

The Barcelona Metropolitan Area (BMA), which includes the capital and 35 surrounding towns, is situated on the shore and is a highly industrialized and densely populated area along the Pre-Coastal and the Coastal Depressions. It is responsible for high pollutant emissions originating from

transportation, industrial, and agricultural activities. One of the most prominent BMA towns along the Besòs and Llobregat rivers is L'Hospitalet de Llobregat, with an important service sector hub. In addition, a gas power station (at Besòs) and two urban waste incinerators (Sant Adrià and a concrete factory at Montcada I Reixac) are also located in this area. Nevertheless, the major sources of atmospheric pollution at the BMA are the road, airport, and shipping traffic emissions (Querol et al. 2001; Rodríguez et al. 2003).

Two mountain chains run parallel to the coast: the Coastal Range and the Pre-Coastal Range. Montserrat and Montseny Massif (1,706.7 m above sea level (m.a.s.l.)) belong to the Pre-Coastal Range, which is longer and higher than the Coastal one: 1000–1500 m.a.s.l. versus 250–500 m.a.s.l. The Central Catalan Depression lies between the Pre-Coastal Range and the Pre-Pyrenees and is suitable for agricultural activities due to its fertile lands. It widens towards the west, linking with the Ebro Depression.

The Vic Plain is located in an intra-mountain 30-km valley embedded in the Catalan Central Depression, 40–70 km northern Barcelona. The most prominent towns of the plain are Vic, Manlleu, and Tona. This region is characterized by a complex orography that, coupled with summer sea breezes and daily anabatic winds, favors the penetration of polluted air masses from the BMA into the Vic Plain and towards the Pyrenees through the north-eastern and western Barcelona valleys (Besòs-Congost valley and Llobregat pathway). Consequently, vertical recirculation and fumigation of O₃-rich air masses prevail in the plain, exacerbated by heatwaves and strong solar radiation in summer (Querol et al. 2017; Massagué et al. 2019; Jaén et al. 2021).

Another industrial center in the Catalan Mediterranean coast is Tarragona, located about 90 km southwest of Barcelona. The town is surrounded by power plants, incinerators, and chemical and petrochemical complexes that spread out until the municipalities of Reus, Salou, and Constantí. The region's orographic and meteorological features bear many resemblances to the summer scenario described for the Vic Plain. Most anthropogenic emissions are located in the Tarragona industrial area and anabatic winds, in conjunction with sea breezes, drive polluted air masses inland until the northern regions of Tarragona province, such as Alcover and Ponts (Jiménez et al. 2005).

Catalonia is bordered in the north by the Pre-Pyrenees and the Pyrenees. These mountainous formations extend approximately 200 km and reach high altitudes (2,000–3,000 m.a.s.l. in case of the Pyrenees). This area includes the air quality stations of Bellver de Cerdanya (1,040 m.a.s.l.), Sort (692 m.a.s.l.), Pardines (1,224 m.a.s.l.), and Montsec (1,676 m.a.s.l.), all located in rural villages and almost no industrial activity, and thus low pollutant emissions. However, in summer, both the eastern and the central parts of the Pyrenees receive anabatic winds in the daytime,

which tend to carry polluted air masses from urban and traffic sites on the coast and central Catalonia towards the mountains (Díaz-de-Quijano et al. 2009; Gonçalves et al. 2009). Apart from these sources of O_3 , high atmospheric altitudes and solar radiation favor O_3 mixing ratios in summer, and minimal local NO emissions hinder O_3 depletion (Ribas and Peñuelas 2006). Therefore, the remote mountainous areas of the Pyrenees are also prone to high O_3 episodes due to the high mixing ratios and meso-meteorological recirculations.

To monitor and control pollution within the CC, the regional government relies on a network of 75 air quality stations, which are included in the Network of Surveillance and Prevention of Air Pollution (Xarxa de Vigilància i Previsió de la Contaminació Atmosfèrica (XVPCA)). Out of all air quality monitoring stations, 18 measure hourly pollution levels for PM_{10} and 44 for O_3 (Fig. 1). Figures 2 and 3 display the location of these air monitoring stations outside the BMA and within the BMA by type (background, industrial, and traffic).

Although XVPCA validates the hourly pollution data, algorithms were programmed in MATLAB, making use of parallel processing and data structures to adapt them to the needs of the calculations. In addition, Tableau was used to

map the different air quality measurement stations and to facilitate the interpretation of the FKT results between stations through spatial analysis.

The CC is one of the most polluted regions within the Western Mediterranean Basin. In 2018, PM_{10} exceedances of the daily values recommended by WHO were recorded in most of the CC, except Alt Llobregat and the Western Pyrenees. The worst records took place in the BMA, Vallès-Baix Llobregat, Central Catalonia, and Vic Plain. In the case of O_3 , all the stations of the air monitoring network, except for a few located in BMA, recorded high exceedances of the 8-h value recommended by WHO (Ecologistas en Acció 2018).

In 22 of the 34 reference stations that assess pollution levels in the CC aimed at the protection of vegetation, the legal objective established for ozone has also been exceeded during the 5 years 2014–2018, affecting mainly crops and forests of Penedès-Garraf, Vic Plain, Comarques de Girona, Alt Llobregat, Eastern Pyrenees, Pre-Pyrenees, Terres de Ponent, and Terres de l'Ebre (Ecologistas en Acció 2018).

Several scientific papers have been written on the behavior of air pollutants within the CC. Querol et al. (2001) described PM_{10} sources at rural, urban, and industrial sites during PM episodes in different local areas around the city

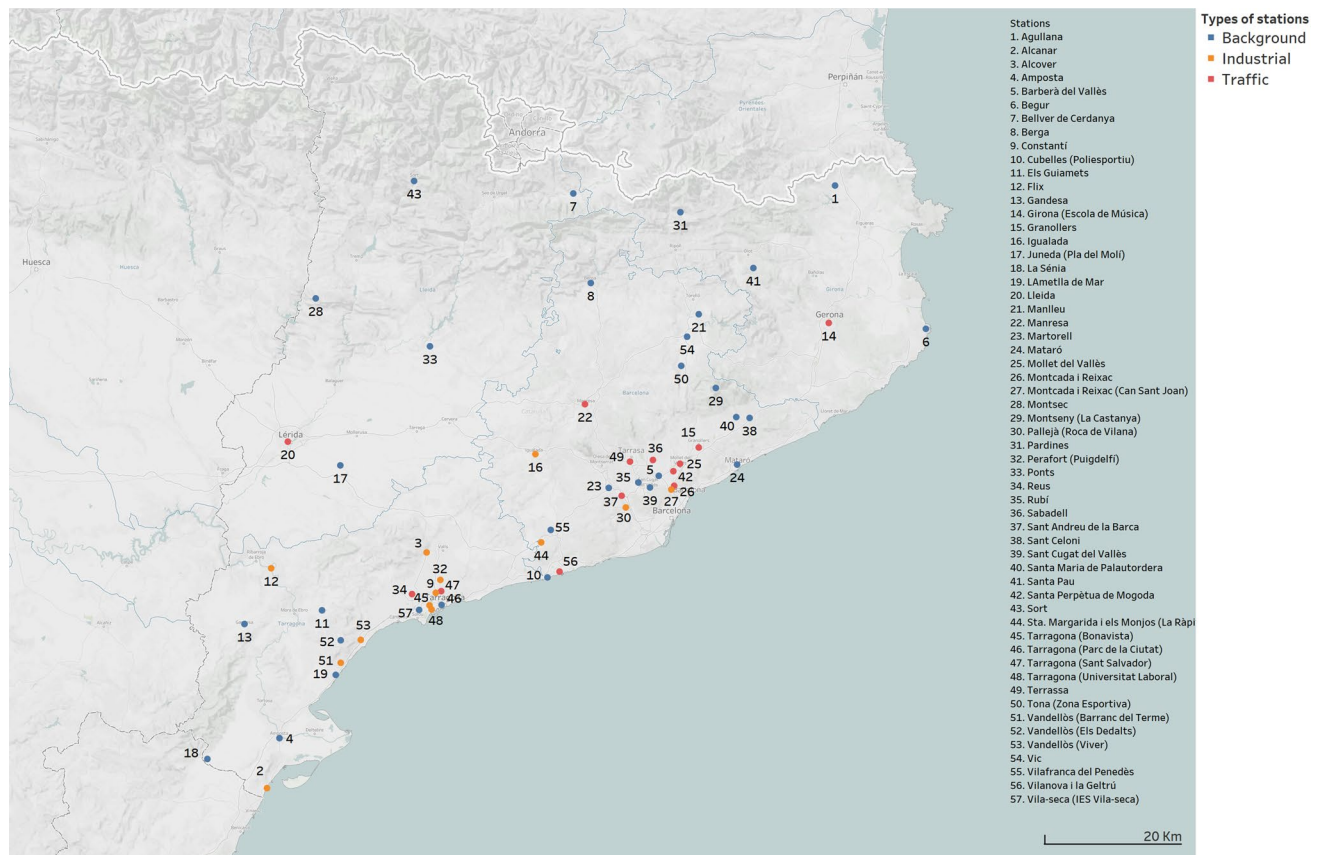


Fig. 1 Distribution of air-quality monitoring stations by type in the CC outside the BMA

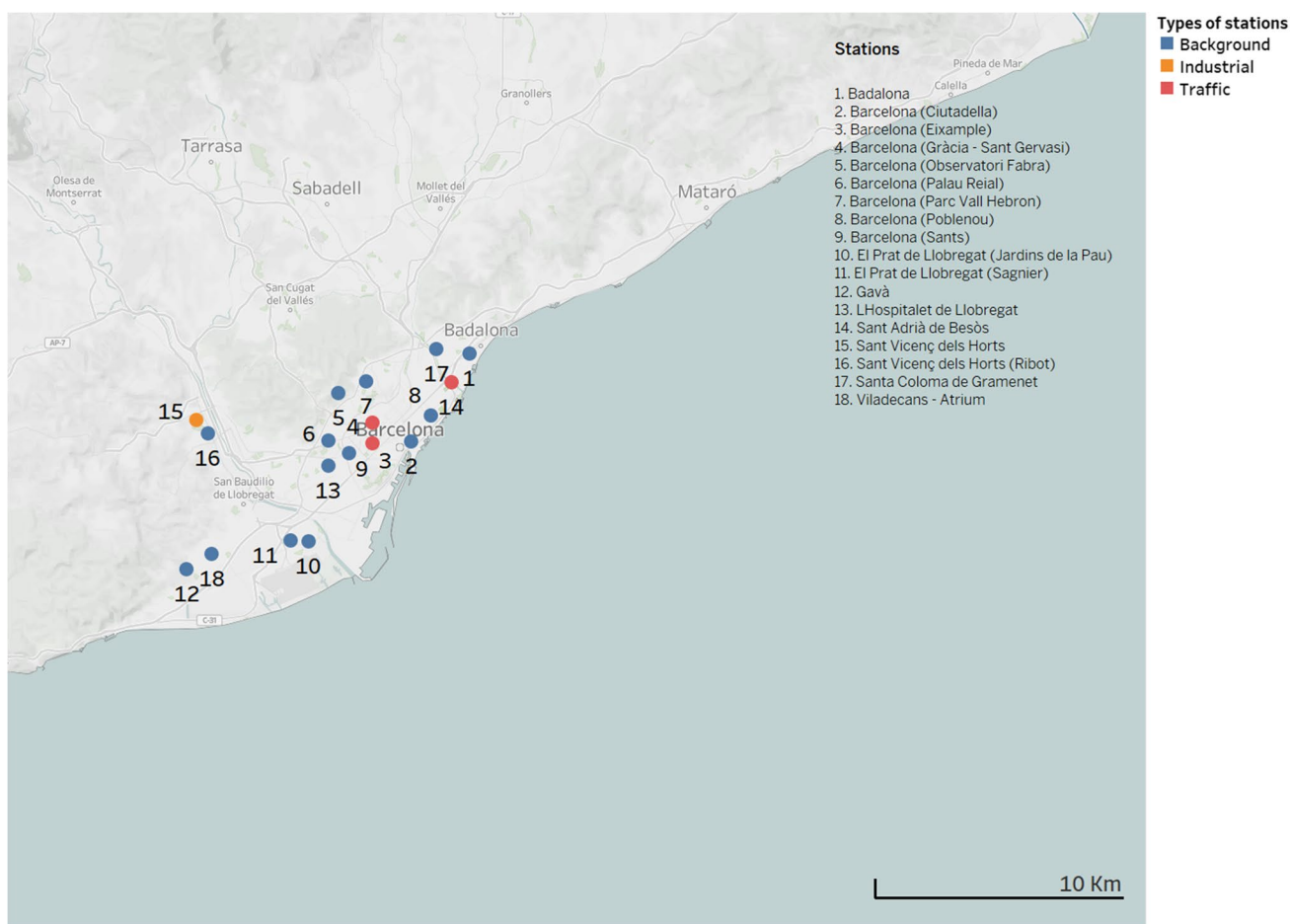


Fig. 2 The 18 air quality monitoring stations of the XVPCA by type—within BMA



Fig. 3 Annual average levels for O₃ (µg·m⁻³) in the period 2013–2020 per station in the CC

of Barcelona. Their results suggest that at rural sites, during the highest daily average PM₁₀ episodes, the main source of pollution is African dust, while vehicle exhaust product is

the major contributor in urban locations. In a related paper, Plasencia-Sánchez et al. (2018) assessed the exposure and health effects of PM in areas of intensive industrial activity

(Tarragona) between 2016 and 2017. They found that the maximum PM concentrations reached $54 \mu\text{g}/\text{m}^3$. Moreover, they pointed out that the areas located far away from the coast shared a similar profile.

Querol et al. (2016) estimated that the contribution of the Barcelona city harbor emissions to the urban background reached 9–12% for PM_{10} and was linked to primary emissions from fuel oil combustion, but also to the developments of secondary ammonium sulfate within the city.

To assess the behavior of O_3 , Massagué et al. (2019) conducted a research in which they analyzed data sets on ozone concentrations in the Vic Plain between 2007 and 2017, the atmospheric basin of Spain that recorded the highest number of exceedances of the hourly O_3 information threshold, frequently affected by the northward transport of atmospheric plume from the BMA. They evaluated how the implementation of short-term measures at a local level could mitigate emission precursors at the BMA. A generalized decrease in regional background O_3 levels was found, together with an increasing trend as far as urban ozone is concerned.

Another recent research developed by Jaén et al. (2020) is related to heatwave-driven ozone episodes in June and July 2019. They pointed out that the phenomenon was characterized by synoptic anticyclonic conditions, surface temperatures over the 98th percentile (over the last 40 years), and high ozone values recorded inland due to precursors' advection (NO_x and VOCs) mainly from BMA, limited by an eastern and a western valley. Moreover, the authors showed that NO_2 measured in Barcelona influenced urban and rural ozone concentrations (100 km from BMA).

Method by statistical analysis

To study the relationships regarding the behavior of O_3 and PM_{10} pollutants between different geographic regions of the CC, this article employs FKT developed by Valencia et al. (2019). This statistic always considers a pair of air quality monitoring stations and measures which periods show similar pollution patterns, and which do not (defined as concordant and discordant periods, respectively). FKT assumes that air pollution levels recorded every hour of the day are discrete observations within the infinite pollution points in time defined by a curve that exhibits continuous behavior.

Because the classification grade according to a total ordering is not a viable option when dealing with functions, the paper is based on pre-orders, the two of which are as follows:

Pre-orders Let us consider the continuous functions g and h on the compact interval $I=[a,b]$

$$f \preceq_m g \equiv \max_{t \in I} f(t) \leq \max_{t \in I} g(t) \tag{1}$$

$$f \preceq_i g \equiv \int_a^b [g(t) - f(t)] dt \geq 0, \tag{2}$$

in which Condition (1), known as the max pre-order, is used to rank functions based on their maximum value, while Condition (2), usually called integral pre-order, is used to order functions based on their underlying area.

This paper follows the second alternative, for it provides more quality information for the study of air contamination. The definitions of functional concordance and functional tau were developed by Valencia et al. (2019).

Functional concordance Let \preceq be a preorder between functions and let $<$ address the case without considering ties. Two pairs of functions (f_1, g_1) and (f_2, g_2) are called functionally concordant if either $f_1 < f_2$ and $g_1 < g_2$ or $f_2 < f_1$ and $g_2 < g_1$. Otherwise, they are called discordant.

Functional Kendall's tau Let $(X_1, Y_1)(X_2, Y_2)$ be two realizations of a bivariate stochastic process $\{(X(t), Y(t) : t \in I)\}$, where $I = [a, b]$. FKT for the population is given by:

$$\tau = [P\{X_1 < X_2, Y_1 < Y_2\} + P\{X_2 < X_1, Y_2 < Y_1\}] - 1 \tag{3}$$

Be $(x_1, y_1) \dots (x_n, y_n)$ of a bivariate random process $(X, Y) = \{(X(t), Y(t) : t \in I)\}$ within the compact interval $I = [a, b]$. Then, the empirical version of FKT is given by

$$\hat{\tau} = \binom{n}{2}^{-1} \sum_{i < j} [2I(x_i < x_j, y_i < y_j) + 2I(x_j < x_i, y_j < y_i)] - 1, \tag{4}$$

where the realizations of the stochastic process are taken as functions. We calculate this statistic by programming Formulas (2) and (4) in MATLAB-R2020.

With the available data, defined generically as L_{psdah} describing the pollution level of pollutant p at air quality measurement station s in the year a , day d , and hour h , the area under the curve of each generated function is calculated by (2). With these results and applying the definition of functional concordance, we use (4) to find FKT. In order not to lose generality $p \in P, s \in S_p, a \in A, d \in D_a, h \in H_p$ where P is defined as the set of pollutants, S_p is defined as the set of air quality stations that measure the pollution levels of particulate p , A is defined as the set of years taken into account for the study, D_a is defined as the total of days in the year a , and H_p is the set defining the number of hours of day where the pollutant p was measured.

When FKT takes value 1, pollution behavior in both air quality stations under study is the same during the observation period. On the other hand, if FKT is equal to -1 , patterns are entirely opposed; in other words, when the levels of a pollutant at a specific air quality station decrease in a year, these levels increase at the other station during the

same year. When FKT is 0, the pollution behavior outlined by the functions is independent. Finally, the statistic FKT is a robust estimator as it exhibits a low sensitivity to outlier data. This characteristic is a significant property in this framework because pollution levels display a large degree of dispersion over time and the time of year. Under the methodology followed by this work, extreme values do not significantly affect the FKT estimates. While other quantitative approaches regard observations as discrete realizations of a random variable, FKT is based on functions to describe daily pollution levels. Thus, it allows us to fully capture the behavioral pattern of a continuous variable during the whole observation period.

Results

Preliminary results

Figures 3 and 4 depict the behavior of O_3 and PM_{10} pollution levels, respectively, within the period 2013–2020. The air quality monitoring stations are ordered from left to right according to their distance from Barcelona city center (the Autonomous Community's capital city), considered the conventional center of the CC. Regarding O_3 , distant stations tend to be located in rural areas such as Ponts, Pardines, Begur, Bellver de Cerdanya, Els Guiamets, Montsec, and La

Senia. These stations tend to display higher pollution levels compared to city centers. However, when it comes to PM_{10} , higher levels stand out in industrial and urban areas, as in Sant Vicenç dels Horts or in Montcada i Reixac—this latter one is located next to Montcada i Reixac's industrial district, called Can Sant Joan. As displayed in Fig. 4, annual mean levels are above those established by WHO (2021), except for Berga and Bellver de Cerdanya.

Even if the scientific community has not yet agreed on an objective threshold above which O_3 and PM_{10} are harmful to people's health, WHO published in September 2021 its updated global air quality guidelines (AQGs) based on more than 500 scientific results. Some of these results associate pollution levels with the exacerbation of certain diseases among adults and children (WHO 2021). In this sense, WHO's new updated pollution limits have set a guideline of $60 \mu\text{g}/\text{m}^3$ as daily 8-h average for O_3 during peak seasons (defined as an average of daily maximum 8-h mean O_3 concentration in the six consecutive months with the highest 6-month running average O_3 concentration), and a $15 \mu\text{g}/\text{m}^3$ annual mean for PM_{10} .

Figure 5a–c show, at some of the CC's most illustrative stations, the number of days per month when average O_3 levels exceeded the recommended short-term (daily maximum 8-h) AQG level for ozone ($100 \mu\text{g}/\text{m}^3$) by WHO (2021) in the period 2013–2020. O_3 levels are calculated as an hourly updated 8-h rolling average. June, July, and August are the months when excess pollution is usually observed. This is

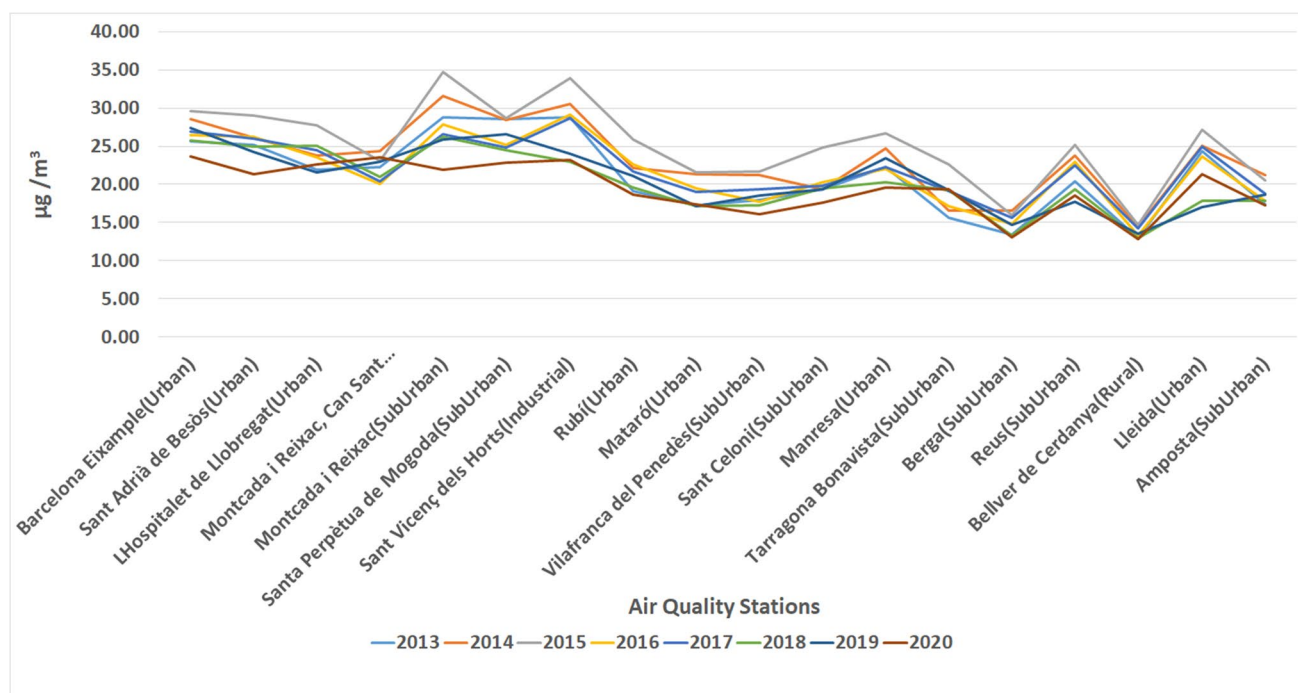


Fig. 4 Annual average levels for PM_{10} ($\mu\text{g}/\text{m}^3$) in the period 2013–2020 per station in the CC

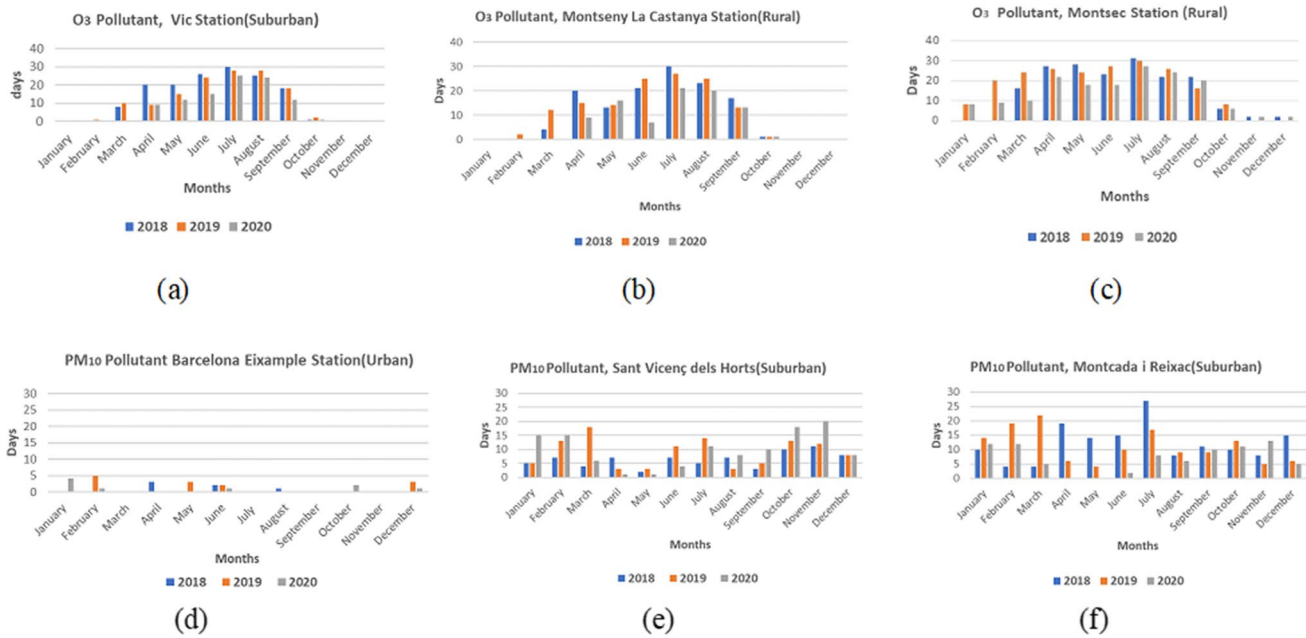


Fig. 5 Several days above the $100 \mu\text{g}/\text{m}^3$ and $45 \mu\text{g}/\text{m}^3$ target values established by WHO for O_3 (a–f)

a very similar pattern to the trend recorded in former years and can be applied to other thresholds too. WHO guideline level exceedances in rural areas of the CC during summer months—particularly between July and August (Valverde et al. 2016)—are not isolated phenomena in rural regions, which means that environmental policies are not yet sufficient to address the problem.

It is worth mentioning that throughout the COVID-induced strict lockdown period (March 15–June 21, 2020) almost all pollutants experienced significant declines due to the standstill of economic activities. Nevertheless, nearly all air quality monitoring stations registered higher O_3 levels compared to the pre-pandemic values, which reveals the challenges for policymaking aimed at achieving the goals proposed by WHO (Betancourt et al. 2021, Morales-Solís et al. 2021).

Pollutant PM_{10} displays a different seasonal pattern than O_3 . Between years 2018 and 2020, the daily average levels exceeded the recommended short-term (24-h) AQG level for PM_{10} ($45 \mu\text{g}/\text{m}^3$) by WHO (2021), particularly in winter (Fig. 5d–f), which justifies that those environmental policies should not be applied in a linear way throughout the whole year but need to take into account each pollutant’s seasonal pattern.

Figures 6 and 7 showcase the mean daily concentration of O_3 and PM_{10} registered in specific Catalan regions based on different types of air monitoring stations according to their geographic location. Figure 6a–d allude to the regions in urban, suburban agglomerations, and rural areas of the CC for pollutant O_3 , while Fig. 7a–d refer to PM_{10} levels at

several air monitoring stations. In each diagram, the period 2018–2019 is reflected, as it stands out for high levels of O_3 and PM_{10} pollutants. During this period, levels of O_3 in urban and suburban areas begin to rise around 8:00 a.m., attain their peak around 17:00, descend until 21:00, and then stay generally stable at night. However, at rural stations, O_3 concentrations start to increase approximately at 10:00 a.m., reach their peak at around 16:00, drop until 22:00, and then stay roughly constant throughout the night. This profile can be observed across charts as meteorological conditions enhance the swift migration of pollutants from urban to rural regions. In addition, the reason why daily levels of O_3 at rural sites within the 2012–2020 period exceeded those of urban sites is the circulation of polluted gases. These exceedances can be witnessed even during the daily maxima.

As for PM_{10} levels, Fig. 7a–d showcase their cyclical daily behavior, consisting in three distinguishable periods: they begin their upward trend around 6:00 a.m., reach their top value approximately at 9:00 a.m., fall until 16:00, start to increase anew at 16:00, get another maximum value at 22:00, and then decline during the night. This pattern may be influenced by the rush hours concentrating more significant movements of people and, therefore, by the use of road transport in the CC.

Kendall functional correlations analysis for O_3

The data collected at each station are represented using eight continuous functions, each showing the daily pollution concentration over a year between 2013 and 2020.

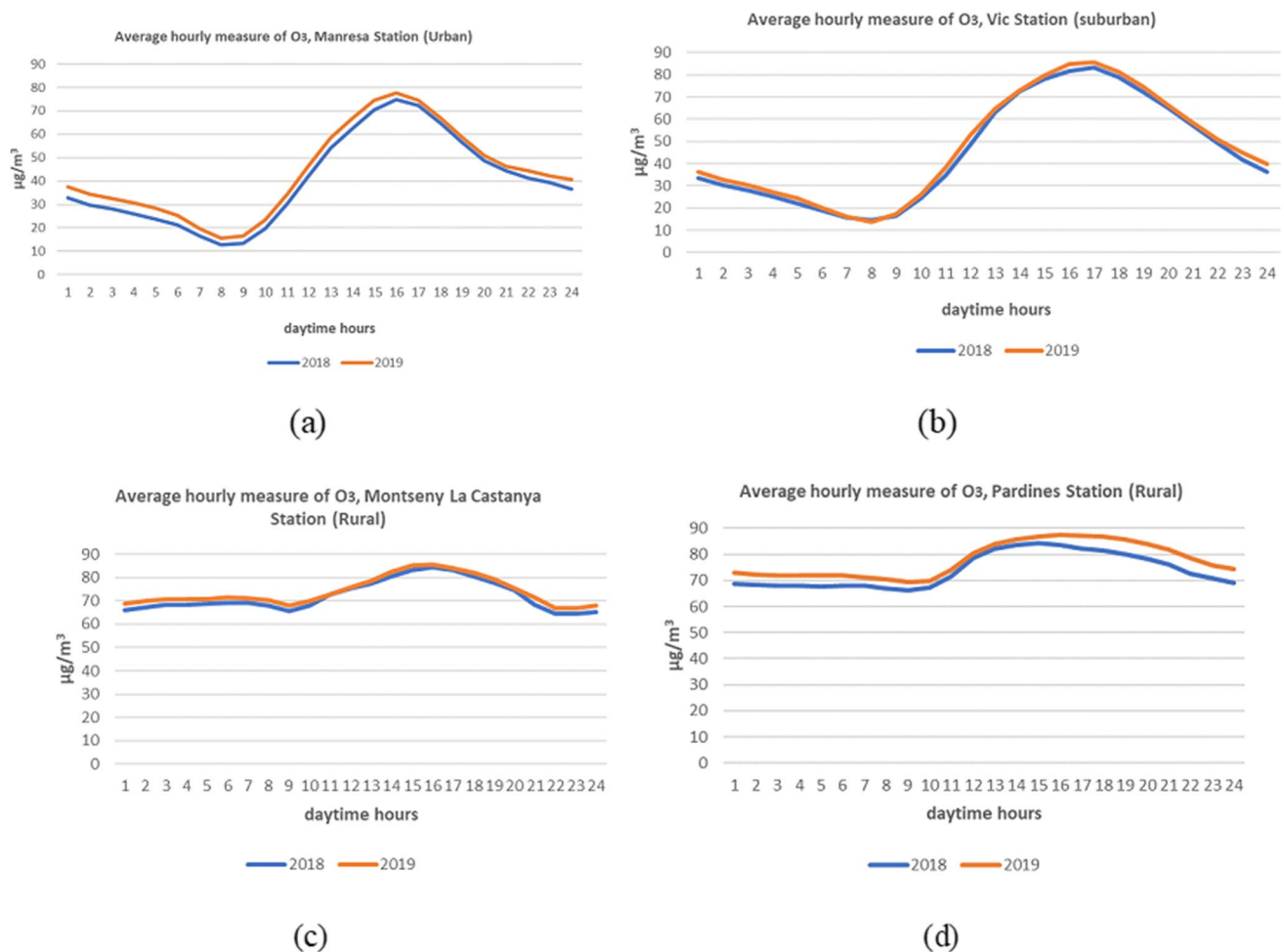


Fig. 6 a–d Hourly average concentrations for O₃ in different areas (urban, suburban, and rural) in the CC during the period 2018–2019

Each continuous function consists of around 364 discrete points, corresponding to daily observations. Subsequently, FKT between pairs of stations is computed, generating a symmetric matrix of correlation coefficients. These values allow us to assess the interaction between different types of stations regarding O₃ and PM₁₀. A positive and a FKT above 0.6 refers to stations whose daily pollution levels feature permanently similar behaviors during the period under analysis. A FKT close to 0 suggests an independence in the daily patterns of pollution levels at the stations being compared.

Figure 8a–d display rural stations located in the northeast of CC and shows their highest and lowest FKTs concerning the rest of the stations. Figures 9–10a–d proceed likewise, choosing other rural stations located in the east and south of CC. The right panel offers a map to outline the location between each rural reference station and the station that is more closely related to its pollution behavior, as measured by FKT. Regarding rural stations located in the northeast, one finds that at most of air quality stations, the station that is most correlated with the rural site is remote (Montsec-Vic,

125.4 km; Pardines-Gavà, 113 km; Bellver de Cerdanya-Vic, 61.4 km; Santa Pau-Vic, 32 km), except for Santa Pau-Vic.

One would expect nearby air quality stations or stations roughly equidistant from the aforementioned rural stations to show similar pollution patterns and have higher or analogous FKTs than those located further away. Such is the case of Reus station, located 105.2 km away from Montsec, which is 20 km less than the distance between Montsec and Vic. Nevertheless, Reus displays a FKT of merely 0.14 with Montsec, while the Montsec-Vic FKT is higher than 0.6. Other examples illustrating this phenomenon take place between Santa Pau and Manlleu, which are only 24 km away from each other, but exhibit a relatively low FKT of 0.43. At the same time, FKT corresponding to Santa Pau and Vic increases to 0.8, even if Vic is located 6 km further from Santa Pau than Manlleu. The distance between Bellver de Cerdanya and Berga is 30 km and these two stations register a FKT of 0.64, whereas Bellver and Vic are 61 km away from each other and record a FKT of 1. In other words, throughout our



Fig. 7 a–d Hourly average concentrations for PM_{10} in different areas (urban, suburban, and rural) in the CC during the period 2018–2019

8-year study period, O_3 pollution behavior among these air quality stations was the same (Fig. 8c).

The stations located in eastern and southern Catalonia exhibit similar patterns as well. The distance between Montseny La Castanya and Berga is merely 55 km and records a FKT of 0.71, whereas FKT corresponding to Montseny-Granollers is 0 even if the stations are within an easy reach of 20 km. Santa María de Palautordera and Vic are separated by 31 km and exhibit a FKT of 0.8, while Santa María de Palautordera and Mataró are only 16.02 km away from each other, and their FKT is 0. The distance between Tona-Berga is 41.3 km and their FKT is 0.71, between La Senia-Constantí 96.5 km and their FKT is 0.64, and between El Guiamets-Berga 143 km and their FKT is 0.71.

These findings indicate that geographical proximity does not explain much about the dynamics of air contamination displayed by different local areas. Quite the contrary, the results signify the existence of latent and complex factors influencing these relationships. To add more clarity on this question, Fig. 10a–c outline the FKT figures regarding the remaining three rural areas of the CC (La Senia, Els Guiamets and Gandesa). Once again, relatively distant locations exhibit higher correlations (La Senia-Constantí, 96.5 km, Els Guiamets-Ampostà 46.5 km,

Gandesa-Ampostà 40 km) according to our findings, whereas lower correlations correspond to closer air quality stations (La Senia-Ampostà, 25.7 km, FKT 0.21; Els Guiamets-Tarragona Parc de la Ciutat, 14 km, FKT – 0.14; and Gandesa-Tarragona Parc de la Ciutat, FKT – 0.07).

A closer review of the results reveals the role played by the Vic and Berga Plains (the former is located close to the Pyrenees and the latter to Barcelona city) and the regions where Reus, Ampostà, and Constantí stations lie (all belong to Tarragona province). In the former area, important farming and agribusiness activities coexist with a diversified industrial fabric and growing retail and service sectors. The Vic air quality station is located at the middle of a flatland called Vic Plain and is roughly equidistant from Barcelona and France. It is characterized by persistent fogs during winter, which often trigger out thermal inversion episodes consisting of minimum temperatures of $-10\text{ }^{\circ}\text{C}$ and maximum temperatures close to $0\text{ }^{\circ}\text{C}$. Storms are regular occurrences in summer and may even invert the Mediterranean climate's typical minimum precipitation levels.

Berga, where the namesake air quality station is located, displays widespread textile, chemical, and machinery industries. Its climate is warm and rainy throughout the whole

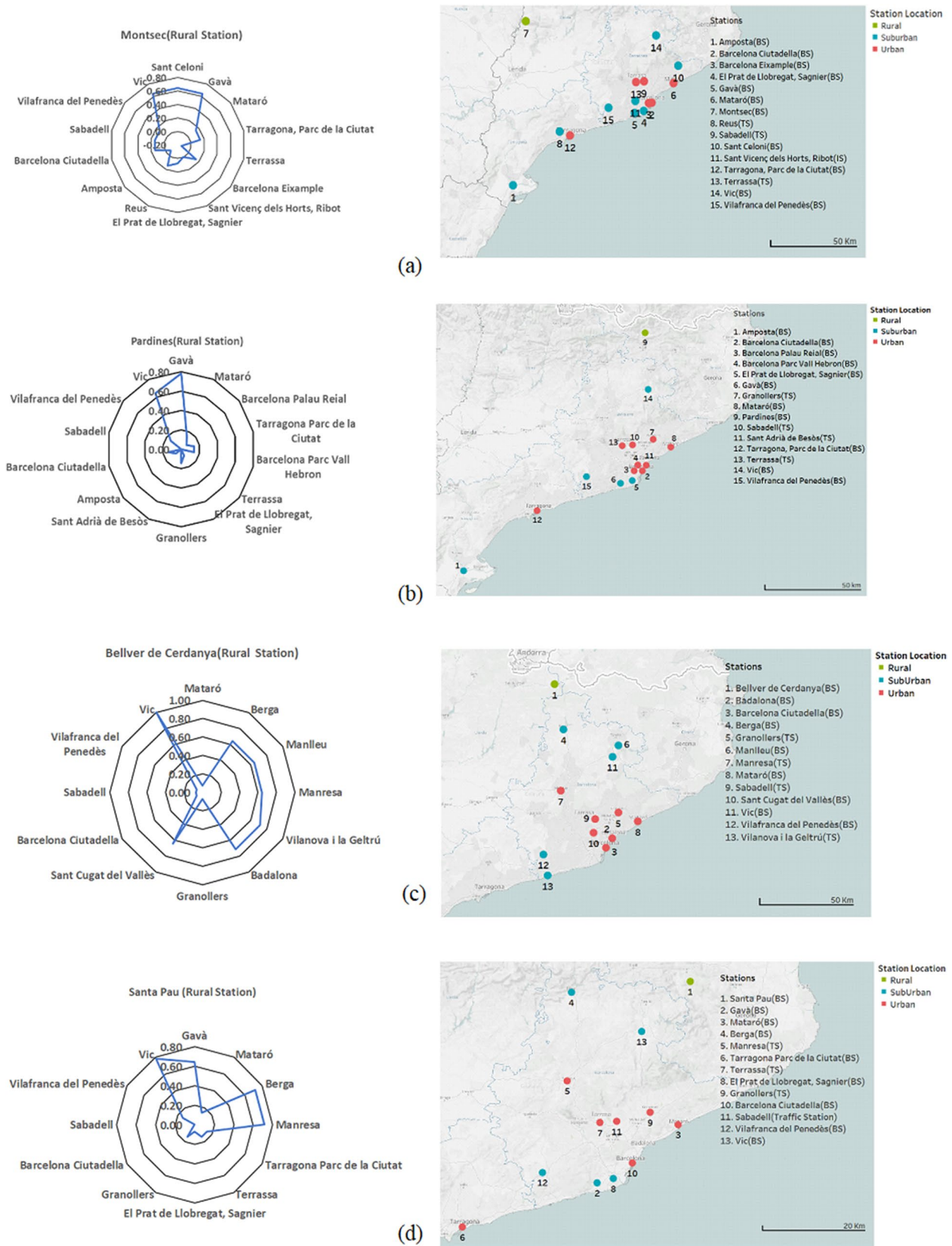
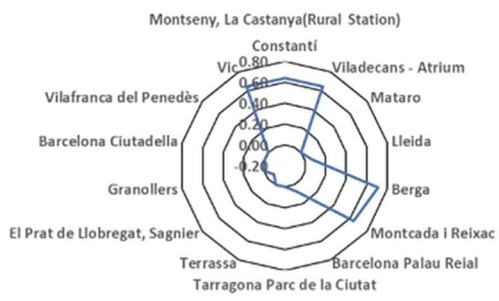
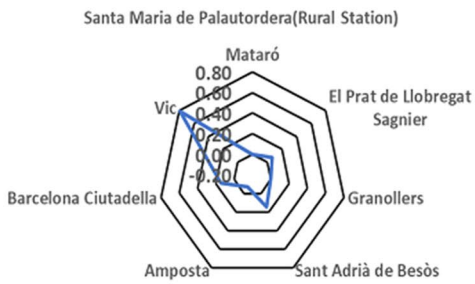
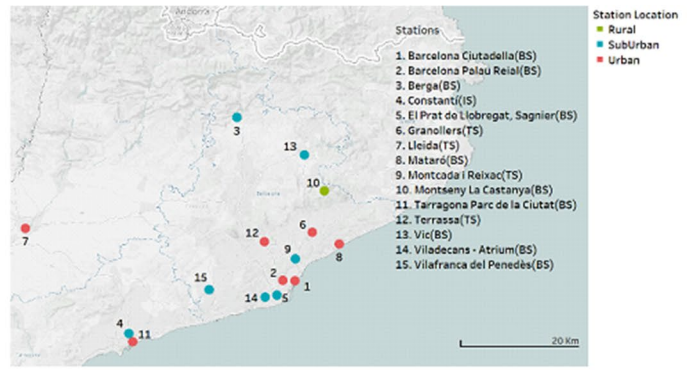


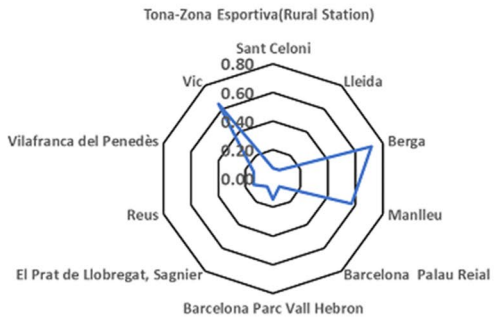
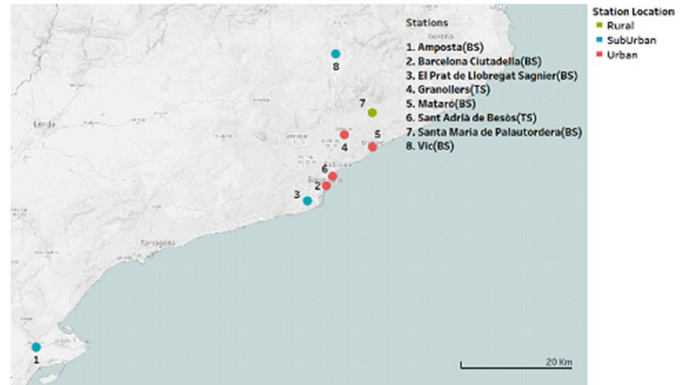
Fig. 8 a–d FKT between rural areas located in the northeast of CC and stations with highest and lowest correlations (2013–2020)



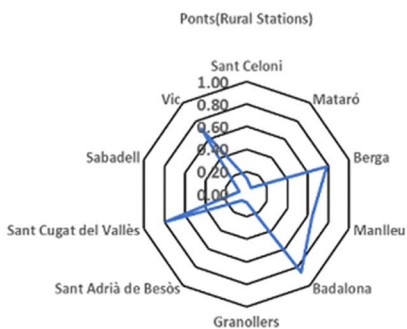
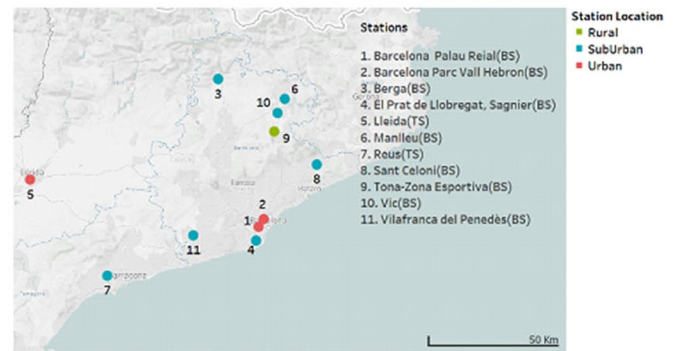
(a)



(b)



(c)



(d)

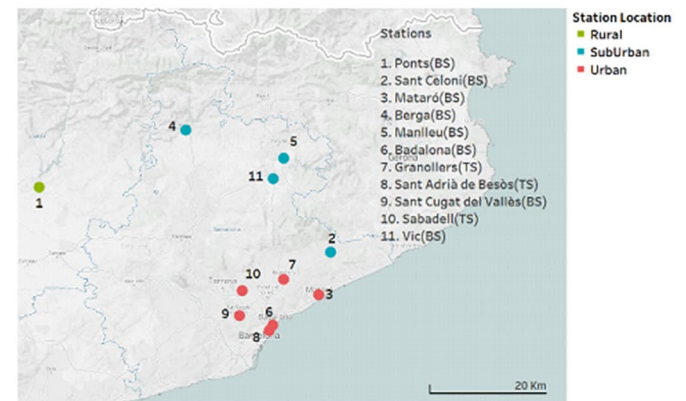
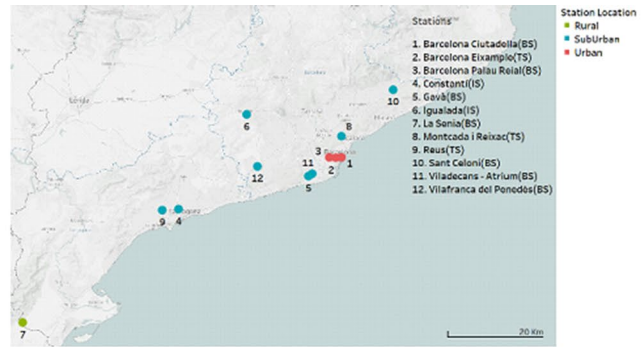
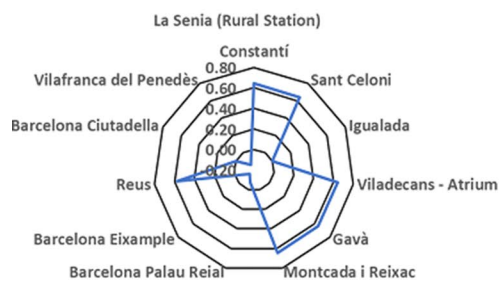
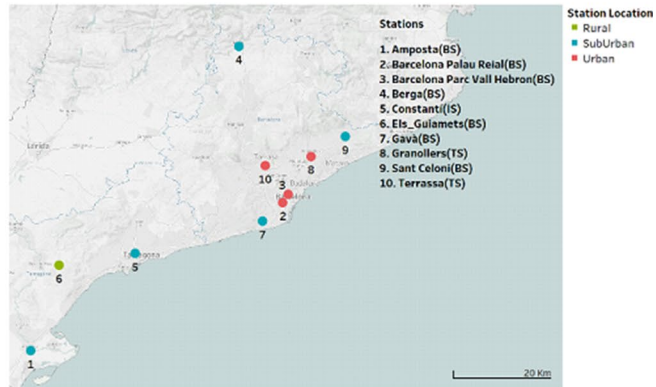
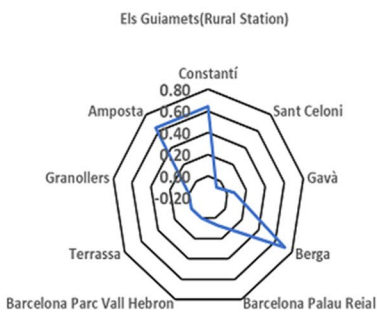


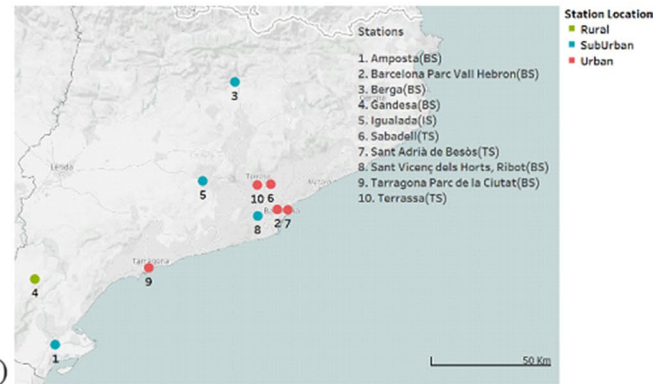
Fig. 9 a–d FKT between rural areas located in the east of CC and stations with highest and lowest correlations (2013–2020)



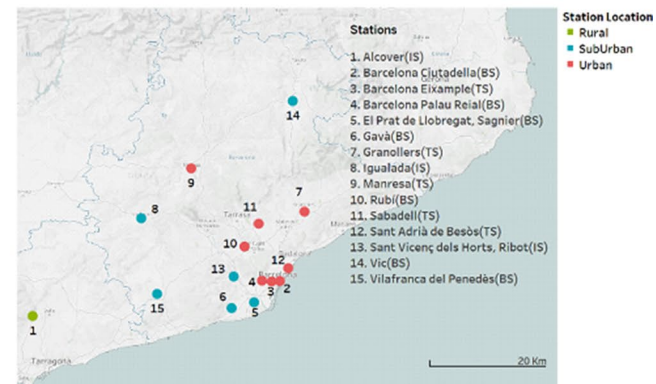
(a)



(b)



(c)



(d)

Fig. 10 a–d FKT between rural areas located in the south of CC and stations with highest and lowest correlations (2013–2020)

year and features some continental patterns due to the presence of mountain ranges that block maritime influence.

The behavior of O₃ pollution at Reus, Amposta, and Constantí stations is likely to reflect the diversified industrial activity carried out in their outskirts, such as petrochemical (one of the most important ones in Spain), metallurgy, and construction sectors.

Therefore, for instance, the data in Fig. 8c and d show an outstanding relationship between two northeastern rural stations (Bellver de Cerdanya and Santa Pau) with Vic, located in the Vic Plain (FKT of 1 and 0.8 respectively). Similarly, Santa María de Palautordera and Tona, located in the east of CC, show a high correlation (0.79 and 0.64, respectively) with Vic, as shown in Figs. 8b–c and 9b–c. Other air quality stations also register high correlation with Berga station, which indicates that pollution patterns are very alike within the districts where these are located. Such is the case of Montseny La Castanya (FKT 0.71, Fig. 9a), Tona (FKT 0.71, Fig. 9c), Els Guiamets (FKT 0.79, Fig. 10b), or Ponts (FKT 0.8, Fig. 9d). This correlation pattern is permanent over time and suggests that O₃ levels in rural areas may be influenced by the Vic and Berga Plains.

A possible answer in line with this behavior is that O₃ generated in Catalan suburban areas, characterized by intense economic activities, spread throughout the entire autonomous community, including remote districts such as Bellver de Cerdanya, Pardines, or Santa Pau, which are among many local tourists' preferred destinations when it comes to leisure and relaxation activities as they are considered the healthiest gateways near Barcelona (Prat and Cànoves 2014; Hernández et al. 2016; Ceballos et al. 2018a, b; Viana et al. 2018; Cors-Iglesias et al. 2020).

Finally, Fig. 11 displays the correlations between non-rural (urban or suburban) sites. The results are very exemplifying. In line with the air mass recirculation pattern outlined in the preceding sections, we find relatively high FKTs between distant sites. For example, a FKT value of 0.71 was found between Mataró and Reus, two urban areas

situated at a distance of more than 100 km from each other. In contrast, the correlation between areas within an easy reach can be significantly low. This is the case of Mataró and Montcada i Reixac, two sites with a FKT below -0.07 and less than 23 km away from each other. These patterns might be caused by the circulatory effects that take place mostly within April–August especially when the wind blows.

Kendall functional correlations analysis for PM₁₀

Figure 12a–d display similarities and dissimilarities, measured by FKT, relative to PM₁₀ pollution patterns in various Catalan municipalities during the period 2013–2020. Air quality stations have been grouped into three categories: urban, suburban, and rural areas.

Just like in the previous figures, the left panel shows at the top the reference air quality station and its highest and lowest FKTs with the remaining stations, whereas the right panel displays a map to locate each air quality station. Regarding traffic stations located at urban sites within the CC, one finds that most of air quality stations with high FKT values are located far away from each other. Such is the case of Santa Perpetua-Manresa (FKT 0.8, see Fig. 12a), 40.91 km; Montcada i Reixac-Reus (FKT 0.8, see Fig. 12b), 96.5 km; Sant Vicenç dels Horts-Reus (FKT 0.8), 78.58 km; and Bellver de Cerdanya-Barcelona Eixample (FKT 0.86, see Fig. 12c), 113.67 km, with the exception of Bellver de Cerdanya-Berga 30.63 km (FKT 0.79).

Montcada i Reixac is a municipality comprised of 34,802 inhabitants, located within the BMA in a river basin flanked by hills. Two dense highways, a cement plant, and a waste treatment facility are found in the area, which considerably contribute to industrial emissions. Moreover, heavy traffic may exacerbate the effect of pollution sources in the nearby environment (Rovira et al. 2018).

On the other hand, Reus is a city belonging to Tarragona province, located the southwest of Barcelona. It features important chemical and petrochemical industries, an



Fig. 11 FKT between urban and suburban areas of CC and stations with the highest and lowest correlations (2013–2020)

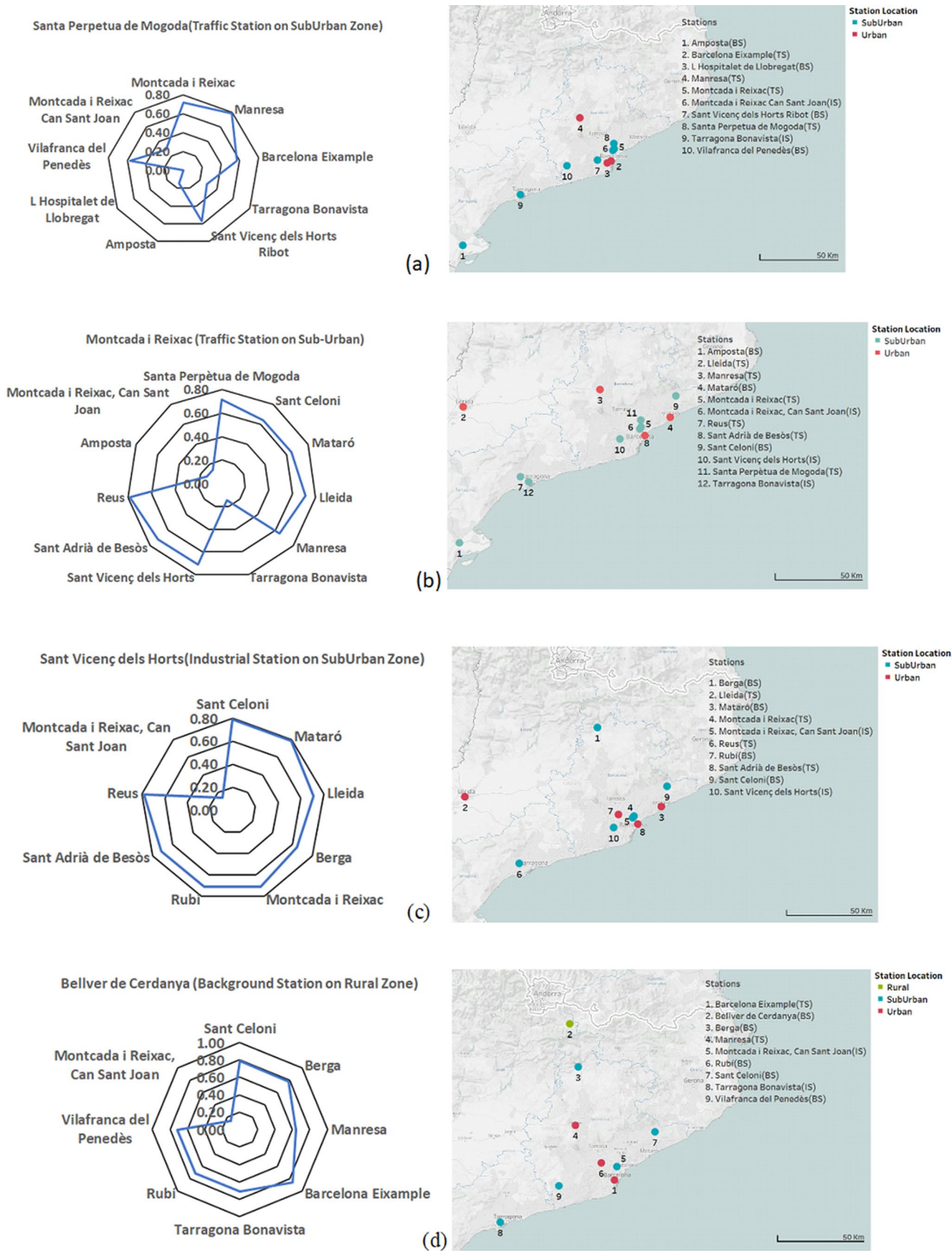


Fig. 12 a–d FKT between stations of CC with highest and lowest correlations for PM₁₀ (2013–2020)

airport, and a growing urban area of 104,373 inhabitants. High air pollution levels in the area are explained by the aforementioned industrial activities in conjunction with the predominant northwest wind that influences the transport of PM₁₀ pollutants (Mari et al. 2016; Mbengue et al. 2017).

The high FKT of 0.8 registered between the previous two sites suggests that PM₁₀ behavior between the years 2013–2020 was very similar. This may be the consequence of several factors: first, both areas' economic activities bear resemblances; second, urban development in both municipalities is alike; and finally, both are affected by complex air mass recirculation patterns.

Sant Vicenç dels Horts is a municipality based on industrial and retail sector development just like the former two sites, contributing to higher average daily PM₁₀ pollution levels through the years (see Fig. 4). Despite a distance of more than 70 km, the fact that FKT correspondent to Reus and Sant Vicenç dels Horts is 0.8 indicates that pollution behaviors are very alike. However, Montcada i Reixac-Can Sant Joan, a station separated by less than 20 km from Sant Vicenç dels Horts, records a FKT of merely 0.14.

The Bellver de Cerdanya rural station is the only one in the CC that records hourly data during the whole 2013–2020 study period, and it recorded the lowest average daily PM₁₀ levels together with Berga station among all 18 stations considered for this study within the same period (see Fig. 4). For the case of Bellver de Cardanya, low PM₁₀ was probably related to local circulations of air masses in the nearby mountain valleys (Jaén et al. 2021). FKT between Bellver de Cerdanya and Berga is 0.8, relatively high. These results prove that using the FKT statistic on functional data allows the detection of sites with similar pollution patterns in the long run, enabling the accurate implementation of specific policies at a local level.

Discussion

Increasing O₃ and PM₁₀ pollution showcases an issue of concern in Catalonia as it jeopardizes citizens' health and the environment (Schembari et al. 2014; Duran et al. 2017; Gamarra et al. 2020; Pierangeli et al. 2020; Rovira et al. 2020). This article focuses on the link between local pollution generated in metropolitan agglomerations and rural areas within the CC. Having observed massive concentrations of O₃ and PM₁₀ in the most peripheral regions of the CC, the article uses functional data in conjunction with an innovative technique by Valencia et al. (2019) to assess the relationship between these two pollutants' levels in urban, suburban, and rural locations.

According to our results, a high degree of pollution between distant areas is revealed, while on occasions, they suggest very mild correlations between nearby sites. These

results prove that the availability of mass data managed through the usage of functional statistics allows the detection of long-term similarities and differences in O₃ and PM₁₀ pollution levels between regions.

Former research featuring molecular organic analysis exhibited higher concentrations of precursors for the formation of ozone at the traffic stations of Barcelona (such as anthropogenic NO₂, which is also an indicator for traffic emissions) compared to rural areas (Jaén et al. 2021). This phenomenon in conjunction with wind direction increases the likelihood of high O₃ records in rural areas in comparison with those sites where ozone precursors are generated. Our findings are consistent with the peculiar redistribution pattern of O₃ particles from urban towards rural areas, and vice versa. In an earlier paper, Gangoiti et al. (2001) found that the local breeze conditions, which are common in summer, contributes to background ozone and circulations of pollutants. Such is the case of Bellver de Cerdanya, where many wind trajectories in this locality passed through Barcelona in the previous hours via Llobregat River Valley as it is outlined in Fig. 12a and b (Jaén et al. 2021). These air mass recirculation dynamics support some of the results outlined in this article. For instance, Bellver de Cerdanya, one of the prominent rural stations considered in the paper, records O₃ maximum values about 1 h after peak O₃ levels are reached at Barcelona Ciutatella, a site located in an urban area where heavy traffic and economic activities are common during the daytime. The delay in the arrival of ozone-loaded air masses produced during the transport of pollution from Barcelona city could explain this phenomenon (Jaén et al. 2021). The succession of the peaks obeys to the typical wind movements in Catalonia, as can be observed in Fig. 13.

According to the results, in general terms, Vic and Berga Plains on the one hand, and Reus, Amposta, and Constantí on the other hand (these latter three embedded in a crucial industrial district within the CC), are regions of influence relative to O₃ concentration. It is suitable to embed this statement within former research that analyzes the interplay between pollution and the CC's climatological and orographic features. The geographic layout of Pardines, Bellver de Cerdanya, or that of the Montsec Range explains their high O₃ records. The arrival of air masses rich in O₃ and its precursors from BMA can be one of the causes of such records, as these air masses are then transported by mesoscale air flows across the valleys connecting the coast to the Pyrenees. When it comes to the rural stations located in the south of Catalonia (Gandesa, Els Guimets, La Senia, and Alcover), the level of O₃ could be attributed to the inflow of high VOC concentrations from industries located in Tarragona (Felipe-Sotelo et al. 2006).

This study offers proof that distance plays a non-linear and complex role relative to O₃ concentrations by generating a pattern of correlations between a wide range of air quality

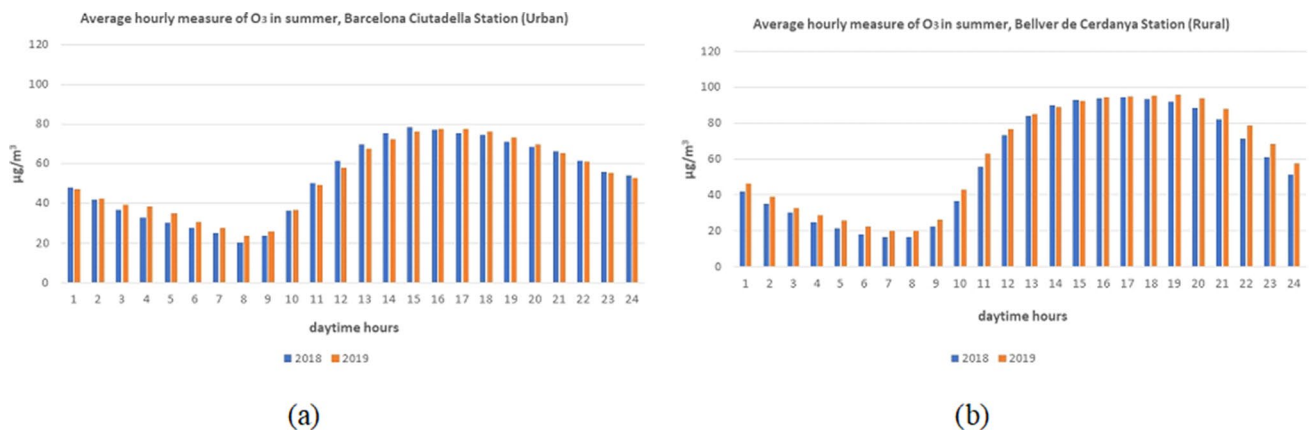


Fig. 13 a, b Average hourly O₃ levels in an urban and a rural district in CC (spring and summer, 2018–2019)

stations located within the CC. Relatively remote urban and rural areas showcase high correlations. In contrast, correlations observed between nearby regions were only moderate, or even non-existent. The profile is attributed to complex air recirculation dynamics influenced by wind flows.

Furthermore, our PM₁₀ pollution analysis revealed that very distant sites record high FKT values and hence show similar features. This phenomenon can be attributed to similarities in population mobility, economic activities, and the influence of air mass circulation patterns (Jaén et al. 2021). For instance, air masses formed in North Africa may carry high PM₁₀ concentrations to the CC, commonly known as Saharan dust episodes. Such is the case of Santa Perpètua de Mogoda or Manresa, both located along the winding paths that arrive at Manresa station between 6:00 and 18:00 h. These wind paths—constructed by recording hourly wind patterns from 2013 to 2020 at climate monitoring station Pont de Vilomara, which lies close to Manresa air quality station—allow us to observe that this area registers winds coming from North Africa in almost 45% of the cases. On the other hand, local air masses could form complex paths transporting PM₁₀ concentrations up to Reus from distant sites like Montcada i Reixac (Jaén et al. 2021). These air mass movements produced at southern coastal regions follow a path that passes through the urban sites of Barcelona city, rise towards northern Manlleu, and then follow a downward route towards the Amposta area. Throughout this complex trajectory, intermediate sites, such as Reus, could be influenced by the winds circulating along the northern areas, which may bring about high PM₁₀ levels. In this sense, it is worth mentioning that almost 30% of the predominant winds in the Reus area come from the north (see Fig. 14b).

Prior research on PM₁₀ at Bellver de Cerdanya station found that pollution levels are low compared to other air monitoring stations located at urban and suburban sites. These results were probably related to local circulations of

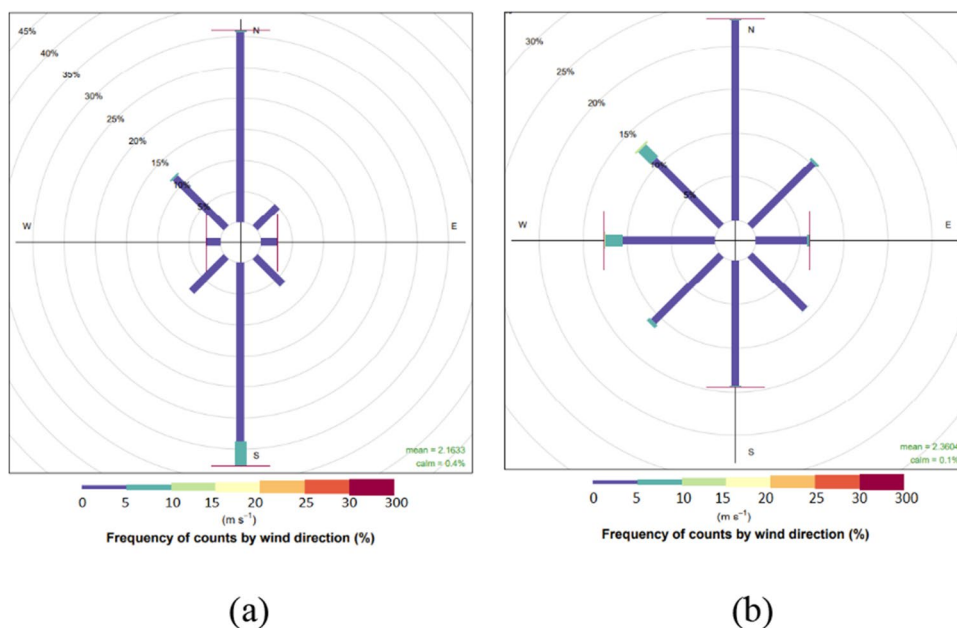
air masses in the nearby mountain valleys (Jaén et al. 2021). Judging by the relatively high FKT value recorded between Bellver de Cerdanya and Berga (0.8), one can deduce that the behavior of PM₁₀ pollution in the Berga region is very similar to that of Bellver de Cerdanya (as observed in Fig. 4). The opposite pattern can be outlined between Bellver de Cerdanya and Montcada i Reixac, Can Sant Joan (FKT of −0.07), suggesting that PM₁₀ levels between these two stations are not related. These results prove that the use of the FKT statistic on functional data allows the detection of sites with similar/dissimilar pollution patterns in the long run, enabling the accurate implementation of specific policies at a local level, not just for one single pollutant, but for any pollutant of interest in the long term.

Conclusions

The process of continuous atmospheric pollution can only be modeled using continuous functions with specific features. This is why functional data coupled with Kendall's functional tau (FKT) was employed throughout this article to analyze the link between O₃ and PM₁₀ pollution between urban, suburban, and rural sites located in the Spanish Community of Catalonia. Despite its potential and popularity in other areas, the application of the FKT method in the analysis of pollution levels among areas is novel. To the best of our knowledge, the present paper is the first one to apply it using data from Catalonia.

The results obtained indicate the existence of complex and non-linear relation between these geographical sites influenced by wind patterns and orography in the CC. In the first place, relatively high FKT coefficients were registered between outlying urban and rural areas regarding O₃, suggestive of similar tropospheric ozone pollution patterns between distant air quality stations. Second, there is a lack

Fig. 14 Wind paths were arriving at Manresa (a) and Reus (b) air quality stations from 6:00 to 18:00 (2013–2020)



of proportionality concerning FKT coefficients and distance between sites. In many cases, distant urban and rural sites exhibited high functional correlation, while some adjacent areas featured low correlations. This phenomenon should be attributed to complex recirculation patterns within the CC. Even if our estimates cannot be interpreted as casual effects, the likelihood that the regions of Reus, Amposta, and Constantí (located in Tarragona province) and the Vic and Berga Plains (an area of intense economic activity in the north of the BMA) exert strong influences on O_3 concentrations at rural sites is high. Moreover, regional wind flows may exacerbate these effects.

As for PM_{10} , high pollution levels at a local level with a positive and high FKT values can be explained by several factors: first, both areas' economic activities bear resemblances; second, urban development in both municipalities is alike; and finally, both are affected by complex air mass recirculation patterns.

The paper was embedded in a functional context, an approach that has rarely been employed. The FKT method provides three main advantages when compared to other quantitative approaches: it is seldom affected by outliers; it does not assume normality for the data of interest; and it can record non-linear relationships. As pollution concentrations, our variable of interest, tend to display a high degree of dispersion over seasons and time, FKT's features are remarkably convenient.

As a handicap, the article does not capture causal effects. The assessment of the impact exerted by a specific air station upon the remaining would demand finding an exogenous source of change in O_3 and PM_{10} levels for each station. Nonetheless, tracing external shocks

that finally impact O_3 and PM_{10} levels in a specific area without affecting the rest of sites is very difficult. Furthermore, it is non-viable to perform this approach given the many areas considered in this article. An additional handicap is the lack of control for orographic and demographic variables in this paper. Arguably, population density, geographical position, transportation, and economic activities may, among other factors, exert a considerable influence on O_3 and PM_{10} levels. More precise correlations between several sites would be registered by considering such factors.

Our results provide two implications for environmental policymaking. In the first place, policymakers should focus on the entire CC when mitigating the adverse effects of pollution, not just Barcelona and Tarragona cities. This implication is based on rural sites' high dependence on polluted air masses generated in urban regions. Secondly, geographical distance is only mildly related to correlations relative to O_3 and PM_{10} levels between regions. Consequently, it may be misleading to use geographical distance to Barcelona or Tarragona cities as a threshold of expected pollution concentrations and peaks at rural sites. The major contribution of the article is the provision of a set of correlations between areas with diverse features within the CC and an outline of empirical air circulation patterns. Public policies whose goal is the mitigation of O_3 and PM_{10} levels among the CC's regions in an equitable way should consider these phenomena in the future.

Funding Not applicable.

Data availability The dataset used in this paper can be download from https://www.miteco.gob.es/es/calidad-y-evaluacion-ambiental/temas/atmosfera-y-calidad-del-aire/calidad-del-aire/evaluacion-datos/datos/Datos_2001_2019.aspx. The correlation data generated during the current study are available from the corresponding author on reasonable request.

Declarations

Ethics approval and consent to participate Not applicable.

Consent for publication Not applicable.

Competing interests The authors declare no competing interests.

References

- Amoatey P, Omid Y, Sicard P, Ahmad S, De-Marco A, Sulaiman H (2021) Temporal incidence and prevalence of bronchitis and morbidities from exposure to ambient PM_{2.5} and PM₁₀. *Environmental Justice* 14(4):267–276. <https://doi.org/10.1089/env.2020.0077>
- Atkinson R (2000) Atmospheric chemistry of VOCs and NO_x. *Atmos Environ* 34(12–14):2063–2101. [https://doi.org/10.1016/S1352-2310\(99\)00460-4](https://doi.org/10.1016/S1352-2310(99)00460-4)
- Auvray M, Bey I (2005) Long-range transport to Europe: seasonal variations and implications for the European Ozone Budget. *J Geophys Res Atmos* 110:D11303. <https://doi.org/10.1029/2004JD005503>
- Betancourt MA, Martínez de Ibarreta Zorita C, Budría Rodríguez S, Wirth E (2021) Local analysis of air quality changes in the community of Madrid before and during the COVID-19 induced lockdown. *Atmosphere* 12(6):659. <https://www.mdpi.com/2073-4433/12/6/659>
- Boudjella A, Saidi F, Hamoudi B, Youcefi A (2017) Evaluation of long range transport of ozone in Western Mediterranean Basin. *Nat Environ Pollut Technol* 16:55–60
- Calfapietra C, Fares S, Manes F, Morani A, Sgrigna G, Loreto F (2013) Role of biogenic volatile organic compounds (BVOC) emitted by urban trees on ozone concentration in cities: a review. *Environ Pollut* 183:71–80. <https://doi.org/10.1016/j.envpol.2013.03.012>
- Castell N, Stein A, Salvador R, Mantilla E, Millán M (2008) The impact of biogenic VOC emissions on photochemical ozone formation during a high ozone pollution episode in the Iberian Peninsula in the 2003 summer season. *Adv Sci Res* 2:9–15. <https://doi.org/10.5194/asr-2-9-2008>
- Ceballos MA, Segura P, Alarcón E, Gutiérrez E, Gracia JC, Ramos P, Reaño M, García B, Villeta C, García M, Aranda JA, Prima H, Veiras X, Bárcena J, García J, Belmonte P, Luengo P, Navascués E, Hernández K (2018a) La calidad del aire en el Estado español durante 2018a. *Ecologistas en Acción*. <https://www.ecologista senaccion.org/96516/informe-la-calidad-del-aire-en-el-estado-espanol-2018a/>. Accessed 15 April 2019
- Cesari D, De Benedetto GE, Bonasoni P, Busetto M, Dinoi A, Merico Chirizzi D, Cristofanelli P, Donato A, Grasso FM, Marinoni A (2018) Seasonal variability of PM_{2.5} and PM₁₀ composition and sources in background site in Southern Italy. *Sci Total Environ* 612:202–213. <https://doi.org/10.1016/j.scitotenv.2017.08.230>
- Chen K, Fiore AM, Chen R, Jiang L, Jones B, Schneider A, Kinney PL (2018) Future ozone-related acute excess mortality under climate and population change scenarios in China: A modeling study. *PLoS Medicine* 15(7). <https://doi.org/10.1371/journal.pmed.1002598>
- Cors-Iglesias M, Gómez-Martín MB, Armesto-López XA (2020) Peer-to-peer accommodation in rural areas of Catalonia: defining typologies of rural municipalities. *Sustainability* 12(15):6145. <https://doi.org/10.3390/su12156145>
- Cristofanelli P, Bonasoni P (2009) Background ozone in the southern Europe and Mediterranean area: influence of the transport processes. *Environ Pollut* 157(5):1399–1406. <https://doi.org/10.1016/j.envpol.2008.09.017>
- Crutzen PA (1973) Discussion of the chemistry of some minor constituents in the stratosphere and troposphere. *Pure Appl Geophys* 106:1385–1399. <https://doi.org/10.1007/BF00881092>
- Dannenmaiera J, Kaltenbacha C, Köllea T, Krischakab G (2020) Application of functional data analysis to explore movements: walking, running and jumping - a systematic review. *Gait Posture* 77:182–189. <https://doi.org/10.1016/j.gaitpost.2020.02.002>
- Dedoussi IC, Eastham SD, Monier E, Barrett Steven RH (2020) Premature mortality related to United States cross-state air pollution. *Nature* 578:261–265. <https://doi.org/10.1038/s41586-020-1983-8>
- Díaz-de-Quijano M, Peñuelas J, Ribas À (2009) Increasing interannual and altitudinal ozone mixing ratios in the Catalan Pyrenees. *Atmos Environ* 43(38):6049–6057. <https://doi.org/10.1016/j.atmosenv.2009.08.035>
- Doherty RM, Wild O, Shindell DT, Zeng G, MacKenzie IA, Collins WJ, Fiore AM, Stevenson DS, Dentener FJ, Schultz MG, Hess P, Derwent RG, Keating TJ (2013) Impacts of climate change on surface ozone and intercontinental ozone pollution: a multi-model study. *J Geophys Res Atmos* 118:3744–3763. <https://doi.org/10.1002/jgrd.50266>
- Duran X, Picó MJ, Reales L (2017) Climate change in Catalonia: executive summary of the Third Report on Climate Change in Catalonia. Government of Catalonia and Institute of Catalan Studies. Barcelona. http://cads.gencat.cat/web/.content/Documents/Publicacions/tercer-informe-sobre-canvi-climatic-catalunya/Resum_executiu_TICCC/RESUM_EXECUT_TICCC_web_EN.pdf. Accessed 12 December 2021
- Ecologistas en Acción (2018) La calidad del aire en el Estado español durante 2017. Madrid. <https://www.ecologistasenaccion.org/97539/informe-la-calidad-del-aire-en-el-estado-espanol-durante-2017/>. Accessed 3 August 2021
- Escudero M, Lozano A, Hierro J, del Valle J, Mantilla E (2014) Urban influence on increasing ozone concentrations in a characteristic Mediterranean agglomeration. *Atmos Environ* 99:322–332. <https://doi.org/10.1016/j.atmosenv.2014.09.061>
- European Environmental Agency (2020) Air quality in Europe-2020 Report No. 09/2020. Luxembourg. <https://www.eea.europa.eu/publications/air-quality-in-europe-2020-report>. Accessed 6 August 2021
- Felipe-Sotelo M, Gustems L, Hernández I, Terrado M, Tauler R (2006) Investigation of geographical and temporal distribution of tropospheric ozone in Catalonia (North-East Spain) during the period 2000–2004 using multivariate data analysis methods. *Atmos Environ* 40(31):7421–7436. <https://doi.org/10.1016/j.atmosenv.2006.07.013>
- Finardi S, Agrillo G, Baraldi R, Calori G, Carlucci P, Ciccioli P, D’Allura A, Gasbarra D, Gioli B, Magliulo V, Radice P, Toscano P, Zaldei A (2018) Atmospheric dynamics and ozone cycle during sea breeze in a Mediterranean complex urbanized coastal site. *J Appl Meteorol Climatol* 57(5):1083–1099. <https://doi.org/10.1175/JAMC-D-17-0117.1>
- Fiore AM, Naik V, Leibensperger EM (2015) Air Quality and Climate Connections. *J Air Waste Manag Assoc* 65(6):645–685. <https://doi.org/10.1080/10962247.2015.1040526>
- Gamarra AR, Lechón Y, Vivanco MG, Garrido JL, Martín F, Sánchez E, Theobald MR, Gil V, Santiago JL (2020) Benefit analysis of the 1st Spanish air pollution control programme on health

- impacts and associated externalities. *Atmosphere* 12(1):32. <https://doi.org/10.3390/atmos12010032>
- Gangoiti G, Millán MM, Salvador R, Mantilla E (2001) Long-range transport and re-circulation of pollutants in the western Mediterranean during the project regional cycles of air pollution in the West-Central Mediterranean Area. *Atmos Environ* 46(8):1230–1251. [https://doi.org/10.1016/S1352-2310\(01\)00440-X](https://doi.org/10.1016/S1352-2310(01)00440-X)
- Generalitat de Catalunya (2021) Territory and people. Barcelona. <https://web.gencat.cat/en/temes/catalunya/coneixer/territori-poblacio/>. Accessed 9 August 2021
- Gonçalves M, Jiménez-Guerrero P, Baldasano JM (2009) Contribution of atmospheric processes affecting the dynamics of air pollution in South-Western Europe during a typical summertime photochemical episode. *Atmos Chem Phys* 9(3):849–864. <https://doi.org/10.5194/acp-9-849-2009>
- Guarin JR, Emberson L, Simpson D, Hernandez-Ochoa IM, Rowland D, Senthold A (2019) Impacts of tropospheric ozone and climate change on Mexico wheat production. *Clim Change* 155:157–174. <https://doi.org/10.1007/s10584-019-02451-4>
- Guo Y, Gasparini A, Armstrong BG, Tawatsupa B, Tobias A, Lavigne E, Coelho MS, Pan X, Kim H, Hashizume M, Honda Y, Guo YL, Wu CF, Zanobetti A, Schwartz JD, Bell ML, Overcenco A, Punnasiri K, Li S, Tian L, Saldiva P, Williams G, Tong S (2016) Temperature variability and mortality: a multi-country study. *Environ Health Perspect* 124(10):1554–1559. <https://doi.org/10.1289/ehp149>
- Hernández JM, Suárez-Vega R, Santana-Jiménez Y (2016) The interrelationship between rural and mass tourism: the case of Catalonia Spain. *Tour Manag* 5443–57. <https://doi.org/10.1016/j.tourman.2015.10.015>
- Hilboll A, Richter A, Burrows JP (2013) Long-term changes of tropospheric NO₂ over megacities derived from multiple satellite instruments. *Atmospheric Chem Phys* 13(8):4145–4169. <https://doi.org/10.5194/acp-13-4145-2013>
- Hopke PK, Dai Q, Li L, Feng Y (2020) Global review of recent source apportionments for airborne particulate matter. *Sci Total Environ* 740:140091. <https://doi.org/10.1016/j.scitotenv.2020.140091>
- Intergovernmental Panel on Climate Change (2014) Climate Change 2013 – the physical science basis: Working Group I Contribution to the Fifth Assessment Report of the Intergovernmental Panel on Climate Change. Cambridge University Press, Cambridge
- Jaén C, Udina M, Bech J (2020) Analysis of two heat wave driven ozone episodes in Barcelona and surrounding region: meteorological and photochemical modeling. *Atmos Environ* 246:118037. <https://doi.org/10.1016/j.atmosenv.2020.118037>
- Jaén C, Villasclaras P, Fernández P, Grimalt JO, Udina M, Bedia C, Drooge BL (2021) Source apportionment and toxicity of PM in urban, sub-urban, and rural air quality network stations in Catalonia. *Atmosphere* 12(6):744. <https://doi.org/10.3390/atmos12060744>
- Jiménez P, Parra R, Baldasano JM (2005) Control of ozone precursors in a complex industrial terrain by using multiscale-nested air quality models with fine spatial resolution (1 km²). *J Air Waste Manag Assoc* 55(8):1085–1099. <https://doi.org/10.1080/10473289.2005.10464709>
- Karthik LB, Sujith B, Rizwan AS, Sehgal M (2017) Characteristics of the ozone pollution and its health effects in India. *Int J Med Public Health* 7(1):56–60. <https://doi.org/10.5530/ijmedph.2017.1.10>
- Klein A, Ancellet G, Ravetta F, Thomas JL, Pazmino A (2017) Characterizing the seasonal cycle and vertical structure of ozone in Paris, France using four years of ground-based LIDAR measurements in the lowermost troposphere. *Atmos Environ* 167:603–615. <https://doi.org/10.1016/j.atmosenv.2017.08.016>
- Largeroy Y, Staquet C (2016) Persistent inversion dynamics and wintertime PM₁₀ air pollution in Alpine valleys. *Atmos Environ* 135:92–108. <https://doi.org/10.1016/j.atmosenv.2016.03.045>
- Lelieveld J, Berresheim H, Borrmann S, Crutzen PJ, Dentener FJ, Fischer H, Feichter J, Flatau PJ, Heland J, Holzinger R, Korrmann R, Lawrence MG, Levin Z, Markowicz KM, Mihalopoulos N, Minikin., Ramanathan V, De Reus M, Roelofs GJ, Scheeren HA, Ziereis H, (2002) Global air pollution crossroads over the Mediterranean. *Science* 298(5594):794–799. <https://doi.org/10.1126/science.1075457>
- Li R, Chow M (2005) Evaluation of reproducibility for paired functional data. *J Multivar Anal* 93(1):81–101. <https://doi.org/10.1016/j.jmva.2004.01.010>
- Lin M, Horowitz LW, Payton R, Fiore AM, Tonnesen G (2017) US surface ozone trends and extremes from 1980 to 2014: quantifying the roles of rising Asian emissions, domestic controls, wildfires, and climate. *Atmos Chem Phys* 17(4):2943–2970. <https://doi.org/10.5194/acp-17-2943-2017>
- Mari M, Sánchez-Soberón F, Audí-Miró C, Van-Drooge BL, Soler A, Grimalt JO, Schuhmacher M (2016) Source apportionment of inorganic and organic PM in the ambient air around a cement plant: assessment of complementary tools. *Aerosol Air Qual Res* 16:3230–3242. <https://doi.org/10.4209/aaqr.2016.06.0276>
- Martínez J, Pastor J, Sancho J, McNabola A, Martínez M, Gallagher J (2020) A functional data analysis approach for the detection of air pollution episodes and outliers: a case study in Dublin. *Ireland Mathematics* 8(2):225. <https://doi.org/10.3390/math8020225>
- Martínez J, Saavedra A, García P, Piñeiro J, Iglesias C, Taboada J, Sancho J, Pastor J (2014) Air quality parameters outliers detection using functional data analysis in the Langreo urban area (Northern Spain). *J Appl Math Comp* 241:1–10. <https://doi.org/10.1016/j.amc.2014.05.004>
- Massagué J, Carnerero C, Escudero M, Baldasano JM, Alastuey A, Querol X (2019) 2005–2017 ozone trends and potential benefits of local measures as deduced from air quality measurements in the north of the Barcelona metropolitan area. *Atmos Chem Phys* 19(11):7445–7465. <https://doi.org/10.5194/acp-19-7445-2019>
- Mbengue S, Alleman LY, Flament P (2017) Metal-bearing fine particle sources in a coastal industrialized environment. *Atmos Res* 183:202–211. <https://doi.org/10.1016/j.atmosres.2016.08.014>
- McDonnell WF, Stewart PW, Smith MV (2010) Prediction of ozone-induced lung function responses in humans. *Inhal Toxicol* 22(2):160–168. <https://doi.org/10.3109/08958370903089557>
- Michelot N, Endlicher W, Carrega P, Martin N, Favez O, Langner M (2016) Impact of a Saharan dust outbreak on PM₁₀ ground levels in Southeastern France. *Climatologie* 12:65–82. <https://doi.org/10.4267/climatologie.1129>
- Millan MM, Mantilla E, Salvador R, Carratalá A, Sanz MJ, Alonso L, Gangoiti G, Navazo M (2000) Ozone cycles in the western Mediterranean basin: interpretation of monitoring data in complex coastal terrain. *J Appl Meteorol* 39(4):487–508. [https://doi.org/10.1175/1520-0450\(2000\)039%3c0487:OCITWM%3e2.0.CO;2](https://doi.org/10.1175/1520-0450(2000)039%3c0487:OCITWM%3e2.0.CO;2)
- Millán MM, Salvador R, Mantilla E (1997) Photooxidant dynamics in the Mediterranean basin in summer: results from European research projects. *J Geophys Res* 102(D7):8811–8823. <https://doi.org/10.1029/96JD03610>
- Monks PS, Archibald AT, Colette A, Cooper O, Coyle M, Derwent R, Fowler D, Granier C, Law KS, Mills GE, Stevenson DS, Tarasova O, Thouret V, von Schneidmesser E, Sommariva R, Wild O, Williams ML (2015) Tropospheric ozone and its precursors from the urban to the global scale from air quality to short-lived climate forcer. *Atmos Chem Phys* 15:8889–8973. <https://doi.org/10.5194/acp-15-8889-2015>
- Morales-Solís K, Ahumada H, Rojas JP, Urdanivia FR, Catalán F, Clar-amunt T, Toro RA, Manzano CA, Leiva-Guzmán MA (2021) The effect of COVID-19 lockdowns on the air pollution of urban areas

- of central and southern Chile. *Aerosol Air Qual Res* 21:200677. <https://doi.org/10.4209/aaqr.200677>
- Orellano P, Reynoso J, Quaranta N, Bardach A, Ciapponi A (2020) Short-term exposure to particulate matter (PM₁₀ and PM_{2.5}), nitrogen dioxide (NO₂), and ozone (O₃) and all-cause and cause-specific mortality: systematic review and meta-analysis. *Environ Int* 142:105876. <https://doi.org/10.1016/j.envint.2020.105876>
- Ortiz-González A, Leeuw-de F, Viana M, Colette A (2018) Air quality in Europe – 2018 Report. European Environment Agency Reports, No 12/2018. <https://www.eea.europa.eu/publications/air-quality-in-europe-2018>. Accessed 15 July 2021
- Paoletti E, De Marco A, Beddows DC, Harrison RM, Manning WJ (2014) Ozone levels in European and USA cities are increasing more than at rural sites, while peak values are decreasing. *Environ Pollut* 192:295–299. <https://doi.org/10.1016/j.envpol.2014.04.040>
- Pierangeli I, Nieuwenhuijsen MJ, Cirach M, Rojas-Rueda D (2020) Health equity and burden of childhood asthma-related to air pollution in Barcelona. *Environ Res* 186:109067. <https://doi.org/10.1016/j.envres.2019.109067>
- Plasencia-Sánchez E, Sánchez-Guijarro M, Sánchez-Soberón F, Rovira J, Sierra J, Schumacher M, Rosell M, Soler A (2018) Particulate matter source apportionment in complex urban and industrial cities: the case of Tarragona, Spain. *WIT Trans Ecol Environ* 230:11–518. <https://doi.org/10.2495/AIR180471>
- Porter WC, Khalil MAK, Butenhoff CL, Almazroui M, Al-Khalaf AK, Al-Sahafi MS (2014) Annual and weekly patterns of ozone and particulate matter in Jeddah, Saudi Arabia. *J Air Waste Manag Assoc* 64(7):817–826. <https://doi.org/10.1080/10962247.2014.893931>
- Prat JM, Cànoves G (2014) Análisis de la evolución de la concentración geográfica de los establecimientos de turismo rural en Cataluña. *Anales De Geografía, Universidad Complutense* 34(1):155–177. https://doi.org/10.5209/rev_AGUC.2014.v34.n1.45196
- Querol X, Alastuey A, Rodríguez S, Plana F, Ruiz C, Cots N, Massagué G, Puig O (2001) PM₁₀ and PM_{2.5} source apportionment in the Barcelona Metropolitan area, Catalonia. *Spain Atmos Environ* 35:6407–6419. [https://doi.org/10.1016/S1352-2310\(01\)00361-2](https://doi.org/10.1016/S1352-2310(01)00361-2)
- Querol X, Alastuey A, Viana M, Rodríguez S, Artíñano B, Salvador P, Santos SG, Patier RF, Ruiz C, Rosa JD, Campa AS, Menéndez M, Gil J (2004) Speciation and origin of PM₁₀ and PM_{2.5} in Spain. *J Aerosol Sci* 35:1151–1172. <https://doi.org/10.1016/j.jaerosci.2004.04.002>
- Querol X, Alastuey A, Reche C, Orio A, Pallares M, Reina F, Dieguez J, Mantilla E, Escudero M, Alonso L, Gangoiti G, Millán M (2016) On the origin of the highest ozone episodes in Spain. *Sci Total Environ* 572:379–289. <https://doi.org/10.1016/j.scitotenv.2016.07.193>
- Querol X, Gangoiti G, Mantilla E, Alastuey A, Minguillón MC, Amato F, Reche C, Viana M, Moreno T, Karanasiou A (2017) Phenomenology of high-ozone episodes in NE Spain. *Atmos Chem Phys* 17(4):2817–2838. <https://doi.org/10.5194/acp-17-2817-2017>
- Querol X, Alastuey A, Gangoiti G, Perez N, Lee HK, Eun HR, Park Y, Mantilla E, Escudero M, Titos G, Alonso L, Temime-Roussel B, Marchand N, Moreta JR, Revuelta MA, Salvador P, Artíñano B, García-dos Santos S, Anguas M, Notario A, Saiz-Lopez A, Harrison RM, Millán M, Ahn KH (2018) Phenomenology of summer ozone episodes over the Madrid Metropolitan Area, central Spain. *Atmos Chem Phys* 18(9):6511–6533. <https://doi.org/10.5194/acp-18-6511-2018>
- Ribas À, Peñuelas J (2006) Surface ozone mixing ratio increase with altitude in a transect in the Catalan Pyrenees. *Atmos Environ* 40(38):7308–7315. <https://doi.org/10.1016/j.atmosenv.2006.06.039>
- Rodríguez S, Querol X, Alastuey A, Mantilla E (2002) Origin of high summer PM₁₀ and TSP concentrations at rural sites in Eastern Spain. *Atmos Environ* 36(9):3101–3112. [https://doi.org/10.1016/S1352-2310\(02\)00256-X](https://doi.org/10.1016/S1352-2310(02)00256-X)
- Rodríguez S, Querol X, Alastuey A, Viana M, Alarcon M, Mantilla E, Ruiz C (2004) Comparative PM₁₀–PM_{2.5} source contribution study at rural urban and industrial sites during PM episodes in Eastern Spain. *Sci Total Environ* 328(1–3):95–113. [https://doi.org/10.1016/S0048-9697\(03\)00411-X](https://doi.org/10.1016/S0048-9697(03)00411-X)
- Rohr AC (2018) Ozone exposure and pulmonary effects in panel and human clinical studies: considerations for design and interpretation. *J Air Waste Manag Assoc* 68(4):288–307. <https://doi.org/10.1080/10962247.2018.1424056>
- Rovira J, Sierra J, Nadal M, Schuhmacher M, Domingo JL (2018) Main components of PM₁₀ in an area influenced by a cement plant in Catalonia, Spain: seasonal and daily variations. *Environ Res* 165:201–209. <https://doi.org/10.1016/j.envres.2018.04.010>
- Rovira J, Domingo JL, Schuhmacher M (2020) Air quality, health impacts and burden of disease due to air pollution (PM₁₀, PM_{2.5}, NO₂ and O₃): Application of AirQ+ model to the Camp de Tarragona County (Catalonia, Spain). *Sci Total Environ* 703:135538. <https://doi.org/10.1016/j.scitotenv.2019.135538>
- Schembari A, Nieuwenhuijsen MJ, Salvador J, de Nazelle A, Cirach M, Dadvand P, Beelen R, Hoek G, Basagaña X, Vrijheid M (2014) Traffic-related air pollution and congenital anomalies in Barcelona. *Environ Health Perspect* 122(3):317–323. <https://doi.org/10.1289/ehp.1306802>
- Seco R, Peñuelas J, Filella I, Llusà J, Molowny-Horas R, Schallhart S, Metzger A, Müller M, Hansel A (2011) Contrasting winter and summer VOC mixing ratios at a forest site in the Western Mediterranean Basin: the effect of local biogenic emissions. *Atmos Chem Phys* 11(24):13161–13179. <https://doi.org/10.5194/acp-11-13161-2011>
- Sillman S, He D (2002) Some theoretical results concerning O₃-NO_x-VOC chemistry and NO_x-VOC indicators. *JGR Atmospheres* 107(D22):ACH 26–1-ACH 26–15. <https://doi.org/10.1029/2001JD001123>
- Striebig B, Smitts E, Morton S (2019) Impact of transportation on carbon dioxide emissions from locally vs. non-locally sourced food. *Emerg Sci J* 3(4):222–234. <https://doi.org/10.28991/esj-2019-01184>
- Valencia D, Lillo RE, Romo J (2019) A Kendall correlation coefficient between functional data. *Adv Data Anal Classif* 13:1083–1103. <https://doi.org/10.1007/s11634-019-00360-z>
- Valverde V, Pay MT, Baldasano JM (2016) Ozone attributed to Madrid and Barcelona on-road transport emissions: characterization of plume dynamics over the Iberian Peninsula. *Sci Total Environ* 543(Pt A):670–682. <https://doi.org/10.1016/j.scitotenv.2015.11.070>
- Van-Drooge BL, Grimalt JO (2015) Particle size-resolved source apportionment of primary and secondary organic tracer compounds at urban and rural locations in Spain. *Atmos Chem Phys* 15(13):7735–7752. <https://doi.org/10.5194/acp-15-7735-2015>
- Viana M, Padrosa M, Querol X, Alastuey A, Benesova N, Krejčí B, Volná V, Real E, Colette A, Leeuw F, González A (2018) Ozone in southern Europe. Assessment and effectiveness of measures, Technical Paper 2017/3. European Topic Centre on Air Pollution and Climate Change Mitigation. https://www.eionet.europa.eu/etcs/etc-atni/products/etc-atni-reports/etcacm_tp_2017_3_ozone_s-europe/@_download/file/ETCACM_TP_2017_3_Ozone_S-Europe.pdf. Accessed 7 February 2021
- Wang T, Xue L, Brimblecombe P, Fat Y, Lam L, Li L, Zhang L (2016) Ozone pollution in China: a review of concentrations, meteorological influences, chemical precursors, and effects. *Sci Total Environ* 575:1582–1596. <https://doi.org/10.1016/j.scitotenv.2016.10.081>
- WHO (2013) Review of evidence on health aspects of air pollution – REVIHAAP Project. Technical Report. World Health Organization, Regional Office for Europe. Copenhagen, Denmark. <https://>

- www.ncbi.nlm.nih.gov/books/NBK361805/ (Accessed 19 July 2021)
- WHO (2015) Economic cost of the health impact of air pollution in Europe: clean air, health and wealth. Copenhagen: WHO Regional Office for Europe. Regional Office for Europe, OECD (2015). http://www.euro.who.int/__data/assets/pdf_file/0004/276772/Economic-cost-health-impact-air-pollution-en.pdf. Accessed August 2020
- WHO (2020) Air Pollution. https://www.who.int/health-topics/air-pollution#tab=tab_1. Accessed 21 September 2020
- WHO (2021) Global air quality guidelines, 2021. Particulate matter PM_{2.5} and PM₁₀, ozone, nitrogen dioxide, sulfur dioxide and carbon monoxide. <https://apps.who.int/iris/bitstream/handle/10665/345329/9789240034228-eng.pdf> (Accessed 30 November 2021)
- Xue L, Gu R, Wang T, Wang X, Saunders S, Blake D, Louie PKK, Luk CWY, Simpson I, Xu Z, Wang Z, Gao Y, Lee S, Mellouki A, Wang W (2016) Oxidative capacity and radical chemistry in the polluted atmosphere of Hong Kong and Pearl River Delta region: analysis of a severe photochemical smog episode. *Atmos Chem Phys* 16(15):9891–9903. <https://doi.org/10.5194/acp-16-9891-2016>
- Yan M, Gong J, Liu Q, Li W, Duan X, Cao S, Li S, He L, Yin Z, Li W, Zhang JJ (2021) The effects of indoor and outdoor air pollution on the prevalence of adults' respiratory diseases in four Chinese cities: a comparison between 2017–2018 and 1993–1996. *J Thorac Dis* 13(7):4560–4573. <https://doi.org/10.21037/jtd-20-2121>
- Yan Y, Lin J, Pozzer A (2019) Trend reversal from high-to-low and from rural-to-urban ozone concentrations over Europe. *Atmos Environ* 213:25–36. <https://doi.org/10.1016/j.atmosenv.2019.05.067>
- Yang J, Tian H, Tao B, Ren W, Pan S, Liu Y, Wang Y (2015) A growing importance of large fires in conterminous United States during 1984–2012. *J Geophys Res* 120(12):2625–2640. <https://doi.org/10.1002/2015JG002965>
- Zong R, Yang X, Wen L, Xu C, Zhu Y, Chen T, Yao L, Wang L, Zhang J, Yang L, Wang X, Shao M, Zhu T, Xue L, Wang W (2018) Strong ozone production at a rural site in the North China Plain: mixed effects of urban plumes and biogenic emissions. *J Environ Sci* 71:261–270. <https://doi.org/10.1016/j.jes.2018.05.003>

Publisher's Note Springer Nature remains neutral with regard to jurisdictional claims in published maps and institutional affiliations.